



Cite this: *Mater. Adv.*, 2021,  
2, 5824

## Surface modification strategies to improve titanium hemocompatibility: a comprehensive review

Vignesh K. Manivasagam,<sup>†a</sup> Roberta M. Sabino,<sup>ID †b</sup> Prem Kantam<sup>a</sup> and Ketul C. Popat <sup>ID \*abc</sup>

Titanium and its alloys are widely used in different biomaterial applications due to their remarkable mechanical properties and bio-inertness. However, titanium-based materials still face some challenges, with an emphasis on hemocompatibility. Blood-contacting devices such as stents, heart valves, and circulatory devices are prone to thrombus formation, restenosis, and inflammation due to inappropriate blood-implant surface interactions. After implantation, when blood encounters these implant surfaces, a series of reactions takes place, such as protein adsorption, platelet adhesion and activation, and white blood cell complex formation as a defense mechanism. Currently, patients are prescribed anticoagulant drugs to prevent blood clotting, but these drugs can weaken their immune system and cause profound bleeding during injury. Extensive research has been done to modify the surface properties of titanium to enhance its hemocompatibility. Results have shown that the modification of surface morphology, roughness, and chemistry has been effective in reducing thrombus formation. The main focus of this review is to analyze and understand the different modification techniques on titanium-based surfaces to enhance hemocompatibility and, consequently, recognize the unresolved challenges and propose scopes for future research.

Received 21st April 2021,  
Accepted 27th July 2021

DOI: 10.1039/d1ma00367d

[rsc.li/materials-advances](http://rsc.li/materials-advances)

### 1. Introduction

Titanium and its alloys have been widely used in blood-contacting devices, such as intra-osseous implants, prosthetic heart valves, cardiovascular stents, and circulatory assist devices.<sup>1</sup> However, improper implant surface interactions with blood are likely to cause thrombosis, and this is a major complication that can lead to the device failure and other serious complications.<sup>2</sup> Thrombosis is an acute syndrome where the blood clots on the implant surface and, once the clotting cascade begins, it spreads rapidly, which can also increase the chances of mortality.<sup>3</sup> To prevent this, patients are prescribed blood thinners such as aspirin, vorapaxar, etc.<sup>4</sup> However, overuse of these medications can weaken the immune system and, during injuries, there is profound bleeding of blood.<sup>5</sup>

Thrombosis is initiated due to the contact of blood to a foreign surface, such as a metal implant surface, and it starts

with the adsorption of blood proteins onto the biomaterial surface, which can lead to a series of complex reactions that ultimately form the thrombus.<sup>6</sup> Studies have shown that there can be thrombus formation and pannus growth in the base of the heart valve struts and apex of the cage, which leads to stenosis, and there is no central flow, which can damage the blood cells (Fig. 1A).<sup>7–9</sup> Another medical device that is usually made of titanium is a left ventricular assist device (LVAD), a mechanical pump that is implanted in a human's chest to assist a weakened heart. The major limitation with these devices is thromboembolism, bleeding, hemolysis, infection, and renal failure. A case study on patients using HeartMate II showed that 11% of the studied patients had thrombus formation in less than one year after implantation (Fig. 1B and C).<sup>10</sup> Infection was also commonly found due to thrombus formation.<sup>10</sup>

In recent years, efforts have been undertaken to reduce the thrombogenicity of biomaterials and therefore prevent these complications.<sup>11</sup> The thrombogenicity of a material is directly related to its surface properties and can be influenced by modifying the surface characteristics such as topography, chemistry, charge, and mechanical properties.<sup>12,13</sup> Therefore, many research groups are focusing on modifying the titanium surfaces to improve their hemocompatibility and prevent the

<sup>a</sup> Department of Mechanical Engineering, Colorado State University, Fort Collins, CO, USA. E-mail: [ketul.popat@colostate.edu](mailto:ketul.popat@colostate.edu)

<sup>b</sup> School of Advanced Materials Discovery, Colorado State University, Fort Collins, CO, USA

<sup>c</sup> School of Biomedical Engineering, Colorado State University, Fort Collins, CO, USA

† These authors contributed equally to this work.





Fig. 1 (A) Thrombus formation around the heart valve frame and strut.<sup>9</sup> Reproduced with permission from ref. 9. Copyright 2016, Elsevier. Examples of thrombosis in a HeartMate II device.<sup>10</sup> (B) Fibrin formation and (C) fibrin with thrombus formation. Reproduced with permission from ref. 10. Copyright 2014, Elsevier.

failure of blood-contacting implants. The aim of this paper is to provide an overview of surface modification strategies that are being applied to improve the blood–surface interaction of titanium-based materials. The paper begins by highlighting the titanium properties (Section 2) and how its surface interacts with blood and its components (Section 3). Then, Section 4 underlines the current progress in surface modification techniques on titanium to enhance its hemocompatibility. Finally, Section 5 concludes the present research work and proposes scopes for future research.

## 2. Titanium and titanium-based alloys

Titanium-based implants have been largely used for biomedical applications due to their excellent mechanical properties, corrosion resistance, and great biocompatibility.<sup>14,15</sup> Titanium has replaced other implant materials such as stainless steel and cobalt–chromium mainly because it has the highest strength–density ratio when compared to all metals, which makes it a light weight implant material of the required strength.<sup>16</sup> In addition, the properties of titanium can be easily modified by forming alloys, making it suitable for a wide range of biomedical applications.<sup>17,18</sup>

Titanium is also well accepted by different body tissues without inducing any negative hypersensitivity, toxicity to the cells, or inflammatory reactions.<sup>19–21</sup> This inert characteristic of titanium is due to its low electrical conductivity.<sup>22</sup> Clinically it has been shown that the body fluids are highly corrosive and many metals like stainless steel, magnesium and chromium–cobalt are degraded quickly due to pitting or fretting corrosion inside the human body.<sup>23</sup> However, metals like titanium oxidize easily, forming a stable thin passivating layer which is self-limiting and protects the implant from further oxidization.<sup>24</sup> These titanium oxide layers are formed at a very fast rate when exposed to moisture in air or water and are usually a few nanometers thick.<sup>25</sup> This oxide layer is shown to be more biologically inert because of its less reactive nature when compared to  $\alpha$ -Ti.<sup>26</sup>

Titanium (Ti) is an allotropic metal.<sup>27</sup> Titanium along with its alloys is classified as  $\alpha$  (low-temperature),  $\alpha + \beta$ , and  $\beta$  (high-temperature) based on the crystal structures present in the substrate.  $\alpha$ -Ti is equated to a hexagonal close packed (HCP)

structure, which endows the alloy with more strength, high fracture toughness and low forgeability.<sup>28</sup> In contrast,  $\beta$ -Ti is when the HCP structure is transformed to a body centered cube (BCC) structure, which makes the metal more ductile (Fig. 2). The temperature at which titanium gets converted from HCP to BCC is 882 °C and is called the beta transus temperature. There are many alloying agents that can change the stabilizing temperature, and based on the application one can change the proportion of  $\alpha$  stabilizing elements (O, Al, N, C) and  $\beta$  stabilizing elements (V, Nb, Mo, Ta, Fe, Mn, Cr, Co, Ni, Cu, Si, H). Addition of alloying agents to pure titanium changes the phase transformation temperatures and stability of the alpha and beta phases. The volume fractions, size, and morphology of the  $\alpha$  and  $\beta$  phases are changed to produce Ti alloys superplastically formable with the potential to design unitized structures for significant weight reduction.<sup>29</sup> This aspect of Ti alloys makes it easy to modify the mechanical properties based on the application. Ti-6Al-4V is an  $\alpha + \beta$  alloy that is ductile and stronger than the  $\alpha$  type or  $\beta$  type Ti alloy. It is important for implants to have both strength and ductility as they will give them a long life under fatigue conditions.<sup>30</sup>

Titanium is often used for medical applications in its pure form or with alloying agents such as vanadium, aluminum, tantalum, nickel, and zirconium.<sup>31</sup> There are four different grades of commercially pure titanium (cpTi) according to the ASTM standards, and these are based on the amounts of oxygen, nitrogen, hydrogen, iron, and carbon during the purification procedures.<sup>32</sup> Among titanium and its alloys, the mainly used materials in the biomedical field are cpTi

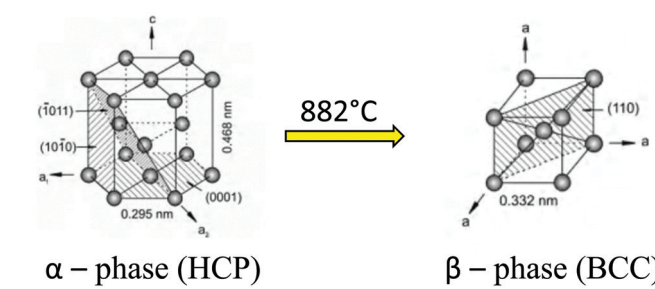


Fig. 2 Crystal structure transformation of titanium.<sup>28</sup> Adapted with permission from ref. 28. Copyright 2013, Elsevier.



(Grade 2), nickel-titanium and Ti-6Al-4V alloys because of their excellent corrosion resistance, low modulus of elasticity, good biocompatibility and high strength.<sup>31</sup> The nickel-titanium alloy has received great attention due to its shape memory feature, which makes it suitable for self-expanding stents.

Even though titanium has outstanding properties required for applications in blood-contacting implants, there are still some complications caused by its surface, such as thrombosis and restenosis.<sup>33</sup> Titanium surface has shown to be highly modifiable at both micro- and nanolevels with simple techniques such as laser treatment, anodization, and hydrothermal treatment, and several studies have shown that these modification techniques can improve the biocompatibility.<sup>20,34,35</sup> Therefore, recent research has focused on different surface modification strategies for titanium and titanium alloys to improve the biomaterial interaction with blood and its components, thus enhancing their hemocompatibility.

### 3. Hemocompatibility of titanium-based biomaterials

Hemocompatibility (*i.e.* blood compatibility) is an essential characteristic for any biomaterial used for blood-contacting medical devices.<sup>36</sup> Blood compatibility is the ability of a material to keep under control the thrombotic and inflammatory responses induced by the foreign surface when in contact with blood.<sup>37,38</sup> These responses correspond to a series of interconnected events that happen on the surface as shown in Fig. 3. Since the interaction between the implant and blood happens only on the implant surface, intensive research has been carried out to develop novel

surfaces that are hemocompatible. Modifying the device surface is effective because it can prevent the blood reactions without altering the favorable bulk material properties.<sup>39</sup>

#### 3.1 Blood-biomaterial surface interactions

**3.1.1 Protein adsorption.** When blood comes in contact with a biomaterial surface, the first event that happens is the adsorption of blood plasma proteins.<sup>40</sup> These blood proteins rapidly form a layer on the biomaterial surface that have a thickness of 2–10 nm and a concentration of proteins that is 1000-fold higher than in blood plasma.<sup>41</sup> This mechanism of protein adsorption is complex and dynamic, and involves electrostatic, van der Waals, and hydrogen bonding interactions.<sup>42</sup> The composition and concentration of adsorbed proteins depend on the physical and chemical properties of the surface and they might change over time, which is known as the ‘Vroman effect’.<sup>43</sup> The Vroman effect is a reversible process wherein the early adsorbed proteins are replaced by proteins that possess higher surface affinity and usually are in relatively lower concentrations in blood.<sup>44</sup> These proteins, once adsorbed to the artificial surface, mediate all the subsequent reactions, such as adhesion and activation of platelets, thrombin generation, complement activation, and adhesion of leukocytes and red blood cells (Fig. 3).<sup>3</sup>

The most abundant proteins in plasma are albumin, immunoglobulins, and fibrinogen.<sup>45</sup> Fibrinogen is a central protein in the coagulation cascade and one of the first to adsorb on biomaterials.<sup>46</sup> Once adsorbed to the artificial surface, it is responsible for platelet and leukocyte adhesion and activation (see Sections 3.1.3 and 3.1.4 for more details).<sup>37</sup> Albumin is generally considered to be inert toward thrombosis, although

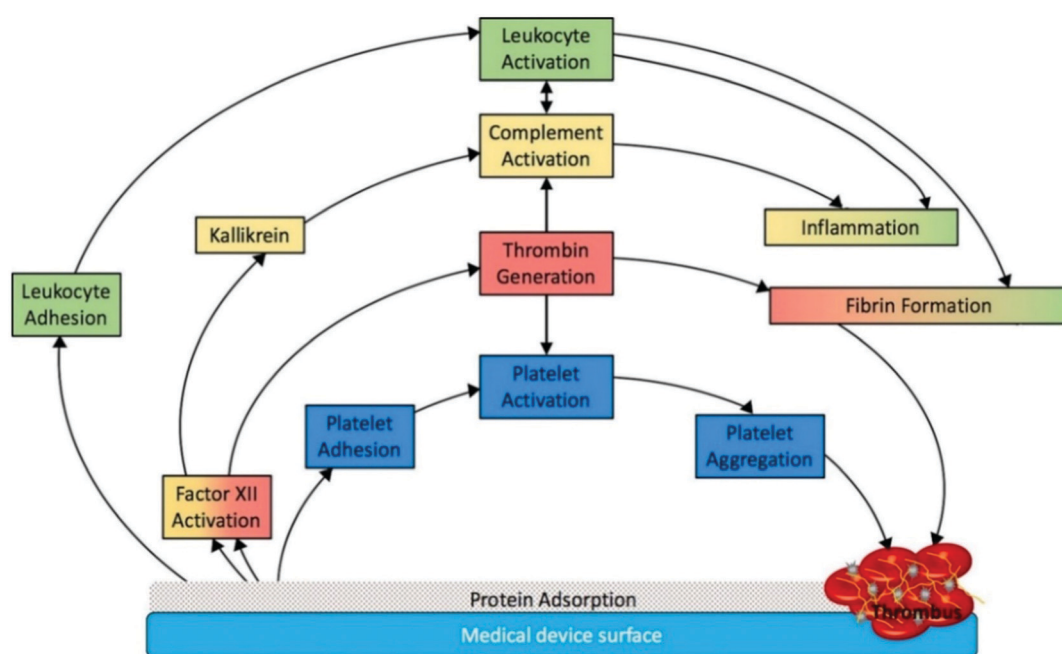


Fig. 3 Schematic representation of medical device associated thrombosis.<sup>5</sup> The initial protein adsorption on the implant surface mediates all the subsequent phenomena. Reproduced with permission from ref. 5. Copyright 2019, Elsevier.



some studies have shown that platelets and leukocytes can adhere to the adsorbed albumin layers.<sup>44</sup> Another key protein involved in thrombus formation is factor XII, which, once activated, triggers a series of complex interconnected reactions.<sup>5</sup>

**3.1.2 Factor XII activation.** Factor XII, also called the Hageman factor, is a plasma protein that autoactivates by adsorption to the biomaterial surface.<sup>47</sup> This autoactivation occurs upon binding with the surface, presumably due to a conformational change, which forms the enzyme FXIIa.<sup>48</sup> FXIIa is then responsible for initiating the intrinsic pathway of coagulation cascade and the complement activation.

**3.1.2.a Coagulation cascade.** The coagulation cascade is the process by which the blood thrombus is formed, and it is divided into two pathways: intrinsic and extrinsic. The extrinsic pathway is triggered by damaged cells in the endothelial tissue, while the intrinsic pathway (also called contact activation) is due to the biomaterial surface interactions with adsorbed proteins.<sup>49</sup> These two pathways are not independent of each other, and both can be involved in the biomaterial-associated thrombosis.<sup>37</sup>

The four proteins involved in the activation of the intrinsic pathway are factor XII (FXII), prekallikrein, factor XI (FXI), and the high-molecular weight kininogen (HMWK). After FXII activation, FXIIa converts prekallikrein into kallikrein and, together with HMWK, activates FXI, producing FXIa.<sup>50</sup> After FXI activation, factor IX is converted to its activated form factor IXa, leading to a cascade of proteolytic reactions that result in thrombin generation by cleavage of prothrombin.<sup>37</sup> Thrombin then converts fibrinogen to fibrin monomers, which polymerize to form the fibrin mesh.<sup>51</sup>

The extrinsic pathway of the coagulation cascade is initiated by tissue factor (TF) expression from damaged cells at the site of vascular injury.<sup>37</sup> Factor VII (FVII) then binds to TF, and after its activation to FVIIa, they form the extrinsic tenase complex: TF-FVIIa complex. The TF-FVIIa complex, in the presence of calcium, cleaves factor X to form factor Xa. After that, both pathways lead to the common pathway where thrombin will be generated and the fibrin mesh will be formed.

**3.1.2.b Complement activation.** In addition, FXII and kallikrein are also involved in triggering the complement activation. The complement system is made up of more than 30 proteins and plays a vital role in the body's immune response.<sup>46,52</sup> The activation of the complement system induced by biomaterials

is part of the inflammatory response and is also interconnected to the coagulation cascade.<sup>37</sup> For example, complement activation is known to occur with vascular grafts, catheters, and during hemodialysis and cardiopulmonary bypass.<sup>5,37</sup>

The complement activation can be initiated by three different pathways: classical, lectin and alternative.<sup>53</sup> Biomaterial surfaces are responsible for triggering both classical and alternative pathways *via* cleavage of FXIIa by kallikrein to produce  $\beta$ -FXIIa.<sup>3</sup>  $\beta$ -FXIIa then activates the classical pathway, and kallikrein activates C3 and C5, generating the reactive fragments C3a and C5a.<sup>5</sup> C3a and C5a might then influence the leukocyte adhesion and activation on the implant surface. These enzymes and reactive fragments generated upon complement activation are also responsible for cell lysis.

**3.1.3 Platelet adhesion.** As mentioned, the adsorbed protein layer plays a vital role in platelet response to biomaterials. The adsorbed fibrinogen mediates the platelet adhesion to the surface, and it varies with the protein conformation changes and the availability of platelet binding domains.<sup>51</sup> Following the platelet adhesion to the implant surface, they undergo a morphological change, resulting in its activation and aggregation. The platelet activation consists of a shape change that produces granule contents and dendrites.<sup>44</sup> These activated platelets then release agonists, such as thromboxane A2 and ADP that intensify platelet adhesion, activation, and aggregation on the medical device.<sup>3</sup>

These platelet-mediated reactions are critical events in thrombus formation and are also interconnected to the intrinsic pathway of blood coagulation.<sup>54</sup> The thrombin generated by the intrinsic pathway also induces more platelet activation and aggregation, which accelerates the coagulation cascade.<sup>55</sup> These platelet aggregates deposited on the implant surface are trapped by the fibrin mesh to form a fibrin–platelet thrombus (Fig. 4).<sup>56</sup> Platelet activation is also known to occur following hemodialysis and cardiopulmonary bypass, and with catheters and vascular grafts.<sup>37</sup>

**3.1.4 Leukocyte adhesion.** Besides the coagulation of blood plasma and the platelet-related reactions, the hemocompatibility of biomaterial surfaces is also influenced by leukocyte activation. Similar to platelets, leukocytes, such as monocytes and neutrophils, can also adhere and activate upon binding to the surface. Fibrinogen is also primarily involved in leukocyte adhesion to biomaterials, and, following activation, the leukocytes can further assist both coagulation and inflammatory processes.<sup>58</sup> The activation of leukocytes has been commonly identified in

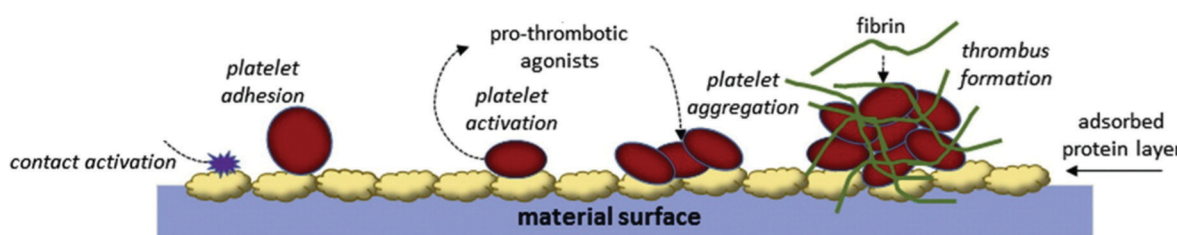


Fig. 4 Platelet adhesion and activation on the biomaterial surface.<sup>57</sup>



cardiovascular devices, such as stents and vascular grafts, as well as during cardiopulmonary bypass, angioplasty, and hemodialysis.<sup>37</sup> Eventually, the monocytes adhered to the implant surface can differentiate into macrophages. These macrophages, once activated, produce pro-inflammatory cytokines that attract more leucocytes.<sup>59</sup> Ultimately, it can lead to the fusion of macrophages to form the giant cells and the recruitment of fibroblasts to form a fibrous capsule. This encapsulation prevents the implant from interacting with the surrounding tissue and can cause the device failure.

### 3.3 Evaluation of the hemocompatibility of titanium surfaces

To achieve good standardization, the methods and models for hemocompatibility tests are described in the ISO 10993-4/2002. Based on the primary process, the hemocompatibility evaluation can be classified into 5 different categories: blood coagulation, immunology, thrombosis, hematology, and platelets (Table 1).<sup>39,60</sup> The evaluation of blood compatibility should also consider that these processes are not isolated and interfere in the other responses.

The coagulation category takes into account the contact activation system (*i.e.*, intrinsic pathway of the clotting cascade). The assays related to it investigate the specific coagulation factors and protein adsorption, as well as the thrombin generation. A previous study has developed a mathematical model that relates coagulation time to FXIIa concentration.<sup>47</sup> It is important to investigate the factor XII activation on titanium biomaterial surfaces as it is responsible for initiating the intrinsic pathway of coagulation cascade and the complement activation. The immunology category covers the study of the complement system and usually focuses on the release of peptide anaphylatoxins (such as C3a, C4a and C5a).<sup>60</sup> The study of thrombosis focuses on the fibrinogen–fibrin conversion and the fibrin mesh formation, while the hematology evaluates leukocyte activation and hemolysis. Hemolysis is the release of hemoglobin from damaged red blood cells (*i.e.* erythrocytes), and it should be below 5%, according to ISO-993-5-10:1992.<sup>62</sup> Another testing method that could be employed to investigate the hemocompatibility of the biomaterial surface is the evaluation of whole blood clotting by a fast hemolysis assay as described elsewhere.<sup>63</sup> The platelet category includes the characterization of platelet adhesion, activation, and agglomeration, as well as its function in the thrombogenic potential of biomaterials.

**Table 1** Hemocompatibility testing (adapted from ISO-10993-4:2002)<sup>61</sup>

ISO 10993-4 categories	Primary process	Assays
Coagulation	Contact activation	Specific coagulation factor Thrombin generation
Immunology	Complement activation	C3a, C5a, iC3b, C4d, SC5b-9 C3 convertase, C5 convertase
Thrombosis	Fibrinogen–fibrin conversion	Percent occlusion and flow reduction
Hematology	Hemolysis	Hemolysis
Platelets	Platelet activation	Leukocyte adhesion/activation Platelet count/adhesion Platelet activation/aggregation

## 4. Strategies for improving hemocompatibility of titanium-based implants

In blood-contacting implants, such as artificial heart valves, cardiovascular stents, and ventricular assist devices, hemocompatibility is crucial. Several studies have established that surface characteristics, such as chemistry, charge, wettability, and topography, play a major role in enhancing blood compatibility.<sup>64–67</sup> Proper surface modification techniques not only maintain the excellent bulk attributes of titanium and its alloys, such as a relatively low modulus, good fatigue strength, machinability, and formability, but also improve specific surface properties demanded by different applications to improve the surface interaction with blood.

### 4.1 Surface properties and their influence on hemocompatibility

Over the last few decades, intensive research has been conducted to understand the physical chemistry behind the biomaterial–blood interaction and how it leads to thrombosis and inflammation. This has promoted significant progress in developing novel surfaces for blood-contacting medical devices. Strategies to enhance the blood compatibility of titanium are based on two main approaches: changing the surface chemistry and topography. By combining both strategies, it is possible to tailor the surface characteristics, such as roughness, wettability, and surface charge, to make the surface more hemocompatible.

When changing the topography, the surface roughness will be affected although roughness is not an exact definition of surface topography since it does not indicate if the roughness dimension is at the macroscale, microscale or nanoscale.<sup>38</sup> The micro/nanoscale architecture attracts great interest in the biomedical field due to the enhanced cellular response and biocompatibility.<sup>25</sup> Surface roughness  $R_a$  is a measure of the finely spaced micro-irregularities on the surface texture and is determined by calculating  $R_a$  and  $R_z$ . While  $R_a$  gives the average surface roughness,  $R_z$  can give information for any pore, hole, or surface deformities detrimental to strength.<sup>68</sup> *In vivo/in vitro* results have shown that surface roughness can influence the protein adsorption, platelet adhesion and activation, and thrombus formation.

While roughness is an important surface property for biomaterial interactions, it is important to understand the



influence of roughness in wetting of the surface. The traditional  $R_a$  and  $R_z$  do not fit well statistically or fractal for superhydrophobic surfaces, which are commonly investigated for blood-contacting applications. On superhydrophobic surfaces there are other phenomena such as pinning of the triple phase line, interface destabilization and wetting transition. Hence, it is essential to study the wettability of the surface.

Surface wettability is an important factor that quantifies how a liquid behaves when it interacts with a solid surface, and this is dictated by the intermolecular interaction of the liquid and solid surface and the cohesive force between the liquid molecules. The surface topography, chemistry, and charge, along with the liquid properties such as polarity, can influence the wettability. Taking the water contact angle ( $\theta$ ) into consideration, surfaces are termed superhydrophilic ( $\theta \sim 0$ ), hydrophilic ( $0^\circ < \theta < 90^\circ$ ), hydrophobic ( $\theta > 90^\circ$ ), and superhydrophobic ( $\theta > 150^\circ$ ). Designing hydrophilic surfaces is desirable as a lower amount of blood plasma proteins adsorb on it in comparison with hydrophobic surfaces.<sup>46</sup> Due to the higher water–surface interaction, hydrophilic surfaces tend to reduce the blood protein adsorption.<sup>69</sup> The wettability of a liquid droplet on a textured surface differs from that on a smooth surface. The measure of macroscopic contact angle on a textured surface is defined as the apparent contact angle which is denoted by  $\theta^*$ . When the liquid droplet comes into contact with a textured surface, it adapts either the Wenzel state or Cassie Baxter state to minimize its overall free energy.<sup>70</sup> In the Wenzel state, the liquid droplet completely penetrates the nano/microtexture of the titanium surface, thereby having a completely wetted interface, and the apparent contact angles are determined by using the relation:

$$\cos \theta^* = r \cos \theta$$

where  $r$  is the surface roughness of the features, which is the ratio of the actual solid liquid interfacial area to the projected surface area.<sup>71</sup> Due to the roughness factor, the Wenzel state enhances wetting or de-wetting based on the Young's contact angle. If  $\theta < 90^\circ$ , then  $\theta^* \ll 90^\circ$ , and if  $\theta > 90^\circ$ , then  $\theta^* \gg 90^\circ$ .

As opposed to the Wenzel state, in the Cassie Baxter state, the droplet does not penetrate the nano/microfeatures due to the pockets of air trapped between the features and the liquid droplet. In the Cassie state the apparent contact angle is determined by using the relation:

$$\cos \theta^* = f_{sl} \cos \theta + f_{lv} \cos(\pi) = f_{sl} \cos \theta - f_{lv}$$

where  $f_{lv}$  is the area fraction of the liquid–vapour interface and  $f_{sl}$  is the area fraction of the solid–liquid interface.<sup>72</sup>

Super-repellent surfaces are surfaces which display high apparent contact angles and low contact angle hysteresis and can be classified into superhydrophobic and superoleophobic surfaces.<sup>70</sup> Superhydrophobic surfaces normally display high apparent contact angles ( $\theta^* > 150^\circ$ ) and low contact angle hysteresis ( $\Delta\theta < 5^\circ$ ) for high surface tension liquids.<sup>70</sup> Super-repellent surfaces are achieved by attaining a Cassie Baxter state of wetting. Once the air is released due to the pressure of the liquid, there is complete wetting, transitioning

from the Cassie state to the Wenzel state which is governed by breakthrough pressure.<sup>73</sup> This transition can make the surface more hydrophilic than the unmodified substrates due to the increase in overall roughness.

The chemical modification of implant surfaces for altering the wettability to reduce thrombus has also been extensively explored. Superhemophobic surfaces (*i.e.* surfaces that repel blood) were developed in recent times to reduce thrombogenicity of blood-contacting devices. These surfaces repel blood *via* a combination of nano/microscale topographies and low surface energy silane coating. The surfaces are coated with various functional groups like  $CF_3$ ,  $CF_2$ , and  $CF_2H$  to lower the overall surface energy of the material, which increases the repellency towards blood. Fluorinated and per-fluorinated materials like per-fluorinated silanes, per-fluorinated phosphates, fluorinated monomers, polymers, and copolymers which have low surface energy have been used to develop hemocompatible materials to reduce thrombosis and improve blood compatibility.<sup>74</sup>

Studies have also explored hydrophilic coating with improved hemocompatibility. Hydrophilic polymers such as poly(ethylene glycol) (PEG) have been used for biomedical applications including bioconjugation, surface modification, and tissue engineering due to critical properties such as good biocompatibility, non-immunogenicity, and resistance to non-specific binding of proteins.<sup>75,76</sup> PEG is very hydrophilic in nature and biochemically inert. PEG chains can be synthesized by controlled polymerization of ethylene glycol or ethylene oxide in aqueous solution.<sup>77</sup> The hydroxyl end groups of the PEG can be replaced by a variety of functional groups to improve the surface properties and enhance the hemocompatibility.<sup>45</sup>

Crystallinity is another surface property that can influence the blood–surface interaction.<sup>78</sup> The  $TiO_2$  on the surface exists in different polymorphs. The phases that have played a major role in biomedical applications are anatase (tetragonal) and rutile (tetragonal).<sup>79</sup> The phase transformation from anatase to rutile leads to a change in the electron structure, thereby modifying the chemical properties of the titanium surface. The rutile phase facets  $\{100\}$  and  $\{110\}$  are thermodynamically stable and hydrophilic due to the molecular adsorption at the O vacancy sites.<sup>80</sup> However, the crystalline  $TiO_2$  is shown to be stable, which is required for a constant biological performance.<sup>81</sup>

## 4.2 Surface modifications on titanium and titanium alloys

As explained in the previous section, the optimization of surface chemistry with micro/nanoscale topography leads to new biomaterials with enhanced hemocompatibility.<sup>38</sup> According to the different clinical needs, various surface modification techniques have been proposed, and this section will focus on these strategies developed in the past few years to improve the hemocompatibility of titanium-based surfaces. An overview on these different strategies is given in Fig. 5.

**4.2.1 Plasma treatment.** A simple technique used to treat titanium surfaces is plasma oxidation. The plasma oxidation treatment is used to generate oxide layers and is considered a green process due to low cost, lower water consumption, and no waste generation.<sup>82</sup> Plasma treatment generally transfers the



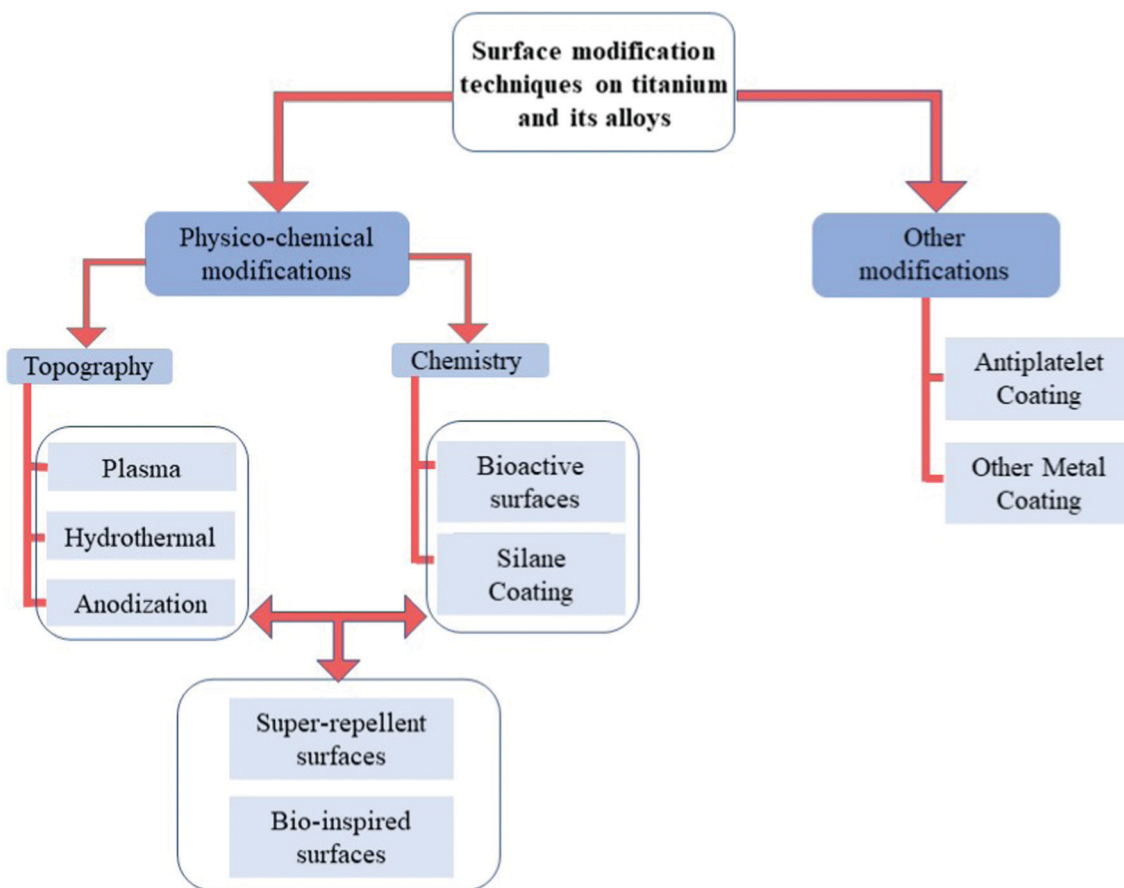


Fig. 5 Different strategies of surface modification on titanium-based surfaces to improve hemocompatibility.

additional energy in the plasma to the surface, increasing the material surface energy and making the surface more reactive.<sup>83</sup> Göttlicher *et al.* investigated the mechanisms required for the formation of nanocrystalline stoichiometric  $\text{TiO}_2$  oxide layers using plasma oxidation.<sup>84</sup> Previous studies have shown that the presence of rutile  $\text{TiO}_2$  phase can reduce thrombosis on the surfaces.<sup>85,86</sup> In addition, the ability to increase the roughness of the oxide layer *via* plasma treatment is also used to modulate the surface hydrophilicity.

Chiang *et al.* showed that the plasma-oxidized samples with a rough dimple-like oxide layer and a nanostructured rutile  $\text{TiO}_2$  phase possess enhanced hemocompatibility.<sup>82</sup> They used oxygen plasma with different treatment powers and durations to modify pure titanium surfaces by oxygen plasma to deposit a titanium oxide layer.<sup>82</sup> The microstructure analysis indicated formation of an island like nanostructured rutile  $\text{TiO}_2$  layer and a dimple like nanostructured rutile  $\text{TiO}_2$  layer on the plasma oxidized titanium surface. The presence of a rough dimple-like oxide layer with nanostructured rutile  $\text{TiO}_2$  indicated better hemocompatibility when compared to control surfaces (Fig. 6A and B).

Hung *et al.* deposited  $\text{TiO}_2$  layers using oxygen plasma immersion ion implantation (oxygen PIII). The oxygen PIII treated surfaces indicated the presence of the  $\text{Ti}^{4+}$  chemical state which consisted of nanocrystalline  $\text{TiO}_2$  with a rutile

structure.<sup>86</sup> The biological studies indicated delayed clotting time on the oxygen PIII treated surfaces which was associated

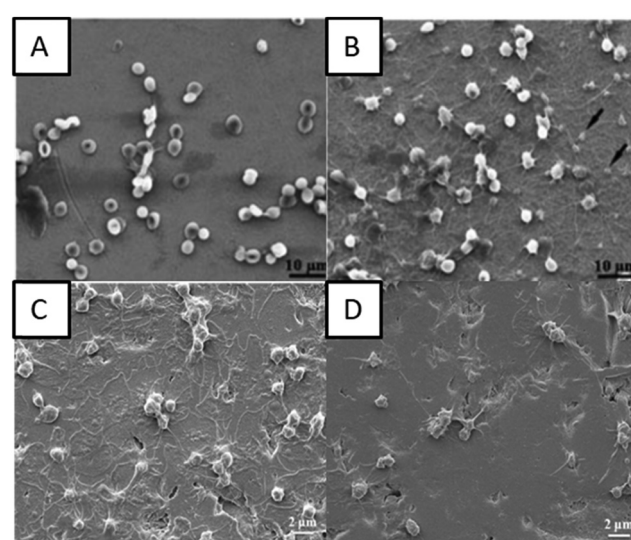


Fig. 6 (A and B) SEM images of red blood cells on control surfaces and plasma oxidized surfaces at 280 W for 30 min, respectively.<sup>82</sup> SEM images showing the interaction of platelets with (C) titanium surfaces and (D) oxygen PIII treated surfaces.<sup>86</sup> Reproduced with permission from ref. 86. Copyright 2016, Elsevier.



with decreased fibrinogen adsorption. The oxygen PIII treated surfaces also showed lower platelet adhesion indicating that the blood compatibility of the titanium implants can be improved by oxygen PIII (Fig. 6C and D).

Klein *et al.* investigated the plasma electrolytic oxidation (PEO) on titanium surfaces by different phosphate-based electrolytes for use in ventricular assist devices (VADs).<sup>87</sup> The PEO coating technique builds up  $\text{TiO}_2$  oxide layers on the surface and is a process similar to alternating current anodizing. Although both processes use a counter electrode and a power supply, the PEO requires higher voltage conditions than anodization, which leads to the development of different surface morphologies.<sup>87</sup> This PEO coating can generate a variety of nanostructures that were able to prevent platelet adhesion and reproduce good hemocompatibility observed in modern VADs, as well as improve the wear resistance of the material.

**4.2.2 Hydrothermal treatment.** Hydrothermal treatment (HT) is a simple process wherein titanium substrates are treated at elevated temperature and pressure, mostly in a liquid medium (acidic/alkaline).<sup>15</sup> This treatment is highly tunable, and the reaction rate and kinetics can be altered by varying the concentration, temperature and pressure. Substrates are chemically etched and studies have shown that various surface features such as nanofibers, nanopores, nanoflowers, nanoneedles, and nanotubes can be developed on titanium surfaces without altering the bulk properties.<sup>88,89</sup> These nanostructures provide a higher surface area and a similar environment to the natural biological system.<sup>34</sup> Since blood cells and their components, such as proteins and minerals, interact with nanoscale extracellular matrix elements, the surface nanotopography can modulate biological responses and stimulate physiological responses.<sup>35,65</sup>

Vishnu *et al.* developed nanoneedles/nanograss on Ti-29Nb substrates using HT with NaOH solution.<sup>90</sup> The surface was superhydrophilic in nature and has shown reduced platelet adhesion and reduced hemolysis rates, thus improved hemocompatibility (Fig. 7A–C). Manivasagam *et al.* have shown that the hydrothermally developed nanopore and nanoneedle surfaces that are hydrophilic in nature have improved hemocompatibility when compared to unmodified surfaces.<sup>91</sup> The nanopore surface that showed superhydrophilicity had the lowest protein adsorption and significantly decreased the platelet and leukocyte adhesion (Fig. 7D–F).

**4.2.3 Anodization.** Anodization is an electrochemical treatment where the substrate to be treated is the anodic part of the electrolytic cell in an electrolytic solution. This treatment is highly tunable, and the reaction rate and kinetics can be altered by varying the anodization potential, electrolytic composition and concentration.<sup>92</sup> Anodization is a quick and inexpensive electrochemical technique to produce an array of  $\text{TiO}_2$  nanotubes on currently implanted titanium-based devices.<sup>93</sup>  $\text{TiO}_2$  nanotubes have attracted considerable attention due to high biocompatibility and osseointegration properties. Recently they have emerged as a good tool for use in cardiovascular applications, such as stents.<sup>35</sup> Various studies have shown that  $\text{TiO}_2$  nanotubes can be produced with ordered alignment using the anodization process on titanium substrates. The dimensions of the nanotubes such as thickness, diameter and length are controllable by altering the pH, voltage, electrolyte composition, and the time of experiment. The diameter of the nanotubes can be varied between 15 nm and 150 nm, and these structures usually make the surface hydrophilic in nature. The size of the nanotubes plays a key role in platelet adhesion. The 15 nm rods lead to higher platelet adhesion when compared to 100 nm rods.<sup>48</sup>

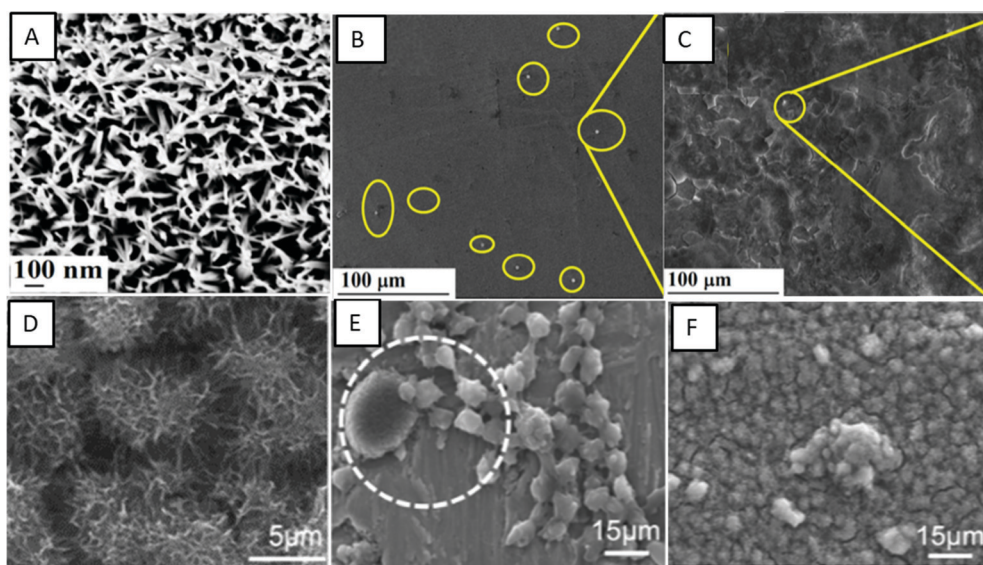


Fig. 7 (A) SEM images showing the surface morphology of hydrothermally treated nanograss surfaces. (B and C) SEM images showing platelet adhesion on control and nanograss Ti29Nb alloy surfaces, respectively.<sup>90</sup> Adapted with permission from ref. 90. Copyright 2020, Elsevier. (D) SEM images showing the morphology of control and hydrothermally treated titanium surfaces, respectively. (E and F) SEM images showing platelets and leukocytes adhered on control and hydrothermally treated titanium surfaces, respectively.<sup>91</sup>



Junkar *et al.* developed nanotubes for stent applications using anodization in hydrofluoric acid solution and further treatment with highly reactive oxygen plasma.<sup>94</sup> Results show that the developed  $\text{TiO}_2$  nanotubes are hydrophilic and have better hemocompatibility compared to unmodified titanium surfaces.<sup>94</sup>  $\text{TiO}_2$  nanotubes treated with plasma decreased platelet and smooth muscle cell adhesion as well as enhanced endothelial cell growth. However, over time the nanotube surfaces were naturally oxidized, which made the surface hydrophobic, thus reducing the hemocompatibility.

Pan *et al.* fabricated  $\text{TiO}_2$  nanotube arrays of varying diameters *via* anodization and further doped them with zinc using hydrothermal treatment to improve biocompatibility.<sup>95</sup> The  $\text{TiO}_2$  nanotube arrays were hydrophilic, whereas the zinc doped  $\text{TiO}_2$  nanotube arrays were superhydrophilic in nature. The hydrophilic and superhydrophilic surfaces increased the albumin adsorption and decreased the fibrinogen adsorption when compared to bare titanium. The results also indicated lower platelet adhesion on the superhydrophilic surfaces (Zn coated  $\text{TiO}_2$  nanotube arrays) when compared to hydrophilic surfaces ( $\text{TiO}_2$  nanotube arrays) and bare titanium (Fig. 8A–C). The zinc coating also reduced the hemolysis rate and enhanced cell compatibility indicating that modified hydrophilic and superhydrophilic surfaces can be used to improve blood compatibility and enhance cell endothelialization.

Gong *et al.* also developed *in situ*  $\text{TiO}_2$  nanotube arrays by anodic oxidation and their crystal structures were further changed by annealing treatment. The effects of  $\text{TiO}_2$  nanotube arrays with different diameters and crystal structures on endothelial cell behavior and blood compatibility were investigated.<sup>96</sup> The results indicated that the  $\text{TiO}_2$  nanotube arrays with a smaller diameter and anatase crystals had good blood and cell compatibility. There was a decrease in the

platelet adhesion and hemolysis rate, while there was also an increase in endothelial cell adhesion and proliferation (Fig. 8D–F).

**4.2.4 Super-repellent surfaces.** Super-repellent surfaces are surfaces that repel most liquids as their surface energy is significantly lower.<sup>97</sup> Although hydrophilicity has been widely employed for blood-contacting medical devices, recent research has shown even lower protein adsorption and platelet adhesion on superhydrophobic surfaces.<sup>98</sup> Superhydrophobicity can be achieved by a combination of surface texture (e.g., micro and/or nanoscale texture) and coating with low surface energy compounds.<sup>99</sup>

Studies have shown that nanotubes that are chemically coated can lead to various surface interactions. Sabino *et al.* showed that when coated with a fluorinated silane the surface was superhydrophobic and when coated with PEG the surface was superhydrophilic.<sup>48</sup> The superhydrophobic surface reduced the amount of protein adsorption and significantly delayed whole blood clotting when compared to other surfaces. Similarly, Xu *et al.* were able to produce a superhydrophobic surface by coating the nanotube surface with self-assembled monolayers of octadecyl phosphonic acid (ODPA).<sup>100</sup>

Jiang *et al.* fabricated superhydrophobic titanium oxide coatings on Ti-6Al-4V alloys by micro-arc oxidation (MAO) treatment and subsequent coating with a 1 wt% alcohol solution of 1H,1H,2H,2H-perfluorooctyl-trichlorosilane (PFOTS).<sup>101</sup> The resulted crater-like porous microstructured superhydrophobic surfaces displayed an apparent water contact angle of 153°. The superhydrophobic surfaces displayed higher corrosion resistance when compared to uncoated Ti-6Al-4V. The superhydrophobic surfaces also showed a low hemolysis ratio and no platelet adhesion, hence improving the blood compatibility of the Ti-6Al-4V alloy (Fig. 9A–C).

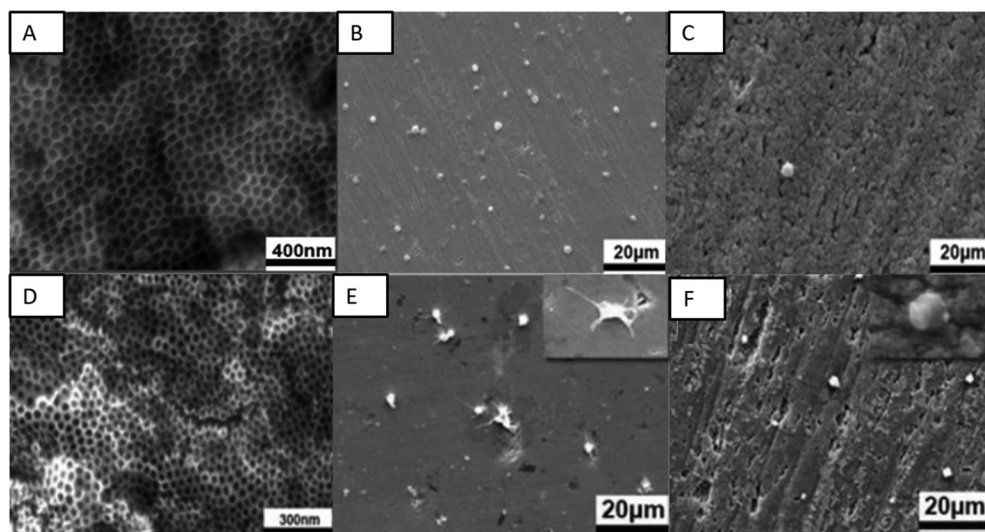
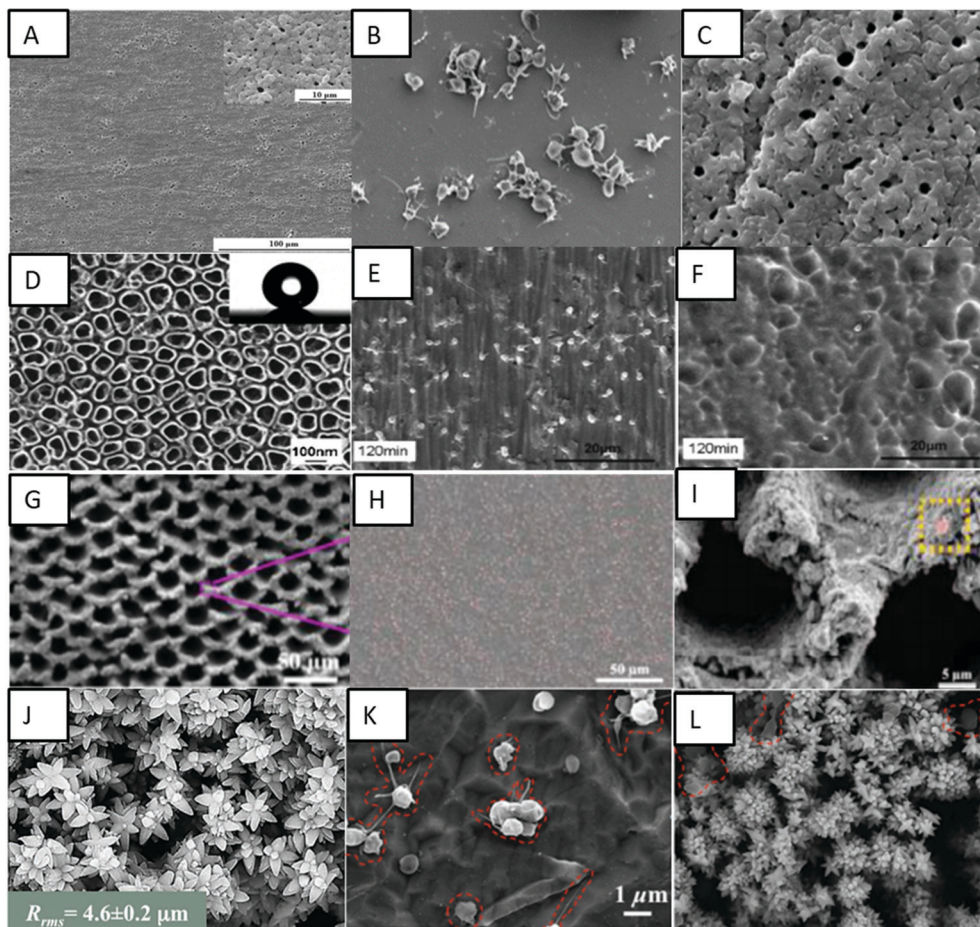


Fig. 8 (A) SEM images showing the surface morphology of zinc doped  $\text{TiO}_2$  nanotubes. (B and C) SEM images showing platelet adhesion on control and zinc doped  $\text{TiO}_2$  nanotubes, respectively.<sup>95</sup> Adapted with permission from ref. 95. Copyright 2020, American Chemical Society. (D) SEM images showing the surface morphology of  $\text{TiO}_2$  nanotube arrays anodized at 30 V. (E and F) SEM images showing platelet adhesion on control and  $\text{TiO}_2$  nanotube arrays (anodized at 30 V).<sup>96</sup> Adapted with permission from ref. 96. Copyright 2019, Elsevier.





**Fig. 9** (A) SEM images showing a crater-like porous microstructure on the Ti-6Al-4V surface. (B and C) SEM images showing platelet adhesion on bare Ti-6Al-4V and superhydrophobic MAO + TFOS surfaces.<sup>101</sup> Adapted with permission from ref. 101. Copyright 2015, Elsevier. (D) SEM image showing superhydrophobic TiO<sub>2</sub> nanotube surfaces. (E and F) SEM images showing platelet adhesion on a bare TiO<sub>2</sub> nanotube surface and a PTES modified superhydrophobic surface, respectively, after 120 min exposure.<sup>103</sup> Adapted with permission from ref. 103. Copyright 2010, Elsevier. (G) SEM image showing multifunctional 3D micro-nanostructures on the nickel–titanium surface. (H and I) SEM images showing platelet adhesion on the pristine nickel–titanium surface and superhydrophobic multifunctional 3D micro-nanostructured surface.<sup>104</sup> Adapted with permission from ref. 104. Copyright 2020, American Chemical Society. (J) SEM images showing nano-flowered surfaces. (K and L) SEM images showing platelet adhesion on non-textured titanium and superhydrophobic nanoflower titanium surfaces.<sup>105</sup> Adapted with permission from ref. 105. Copyright 2016, Wiley-VCH.

Chen *et al.* fabricated a superhydrophobic surface on the Ti-6Al-4V alloy using hydrothermal treatment with NaOH and subsequent coating with PFOTS.<sup>102</sup> Various NaOH concentrations were used to analyze the difference in surface properties. The treatment developed feather-like or grass-like nanostructures on the surface based on the concentration. The coating made the grass-like structure surface superhydrophobic with the highest apparent water contact angle of 159°. The superhydrophobic surface showed a decreased hemolysis ratio, platelet adhesion and a prolonged coagulation time, hence improving the *in vitro* hemocompatibility of the Ti-6Al-4V alloy.<sup>102</sup>

Yang *et al.* fabricated superhydrophobic TiO<sub>2</sub> nanotubes *via* electrochemical anodization in 0.5 wt% HF electrolyte and subsequent coating with a methanolic solution of hydrolyzed 1 wt% 1*H*,1*H*,2*H*,2*H*-perfluoroctyl-triethoxysilane (PTES).<sup>103</sup> The PTES modified TiO<sub>2</sub> nanotubes displayed an apparent water contact angle of 156°. The superhydrophobic nanotube surfaces displayed lower platelet adhesion and activation when

compared to bare titanium and superhydrophilic surfaces, thus exhibiting enhanced hemocompatibility (Fig. 9D–F).

Ma *et al.* fabricated multifunctional 3D microstructures on nickel–titanium alloys using femtosecond laser ablation combined with further fluorination of these microstructures to form a superhydrophobic coating.<sup>104</sup> These fluorinated microstructures displayed an apparent contact angle of 167° for water droplets, indicating superhydrophobicity. The biocompatibility studies have shown a low hemolysis ratio, low platelet adhesion and 100% cell viability on these surfaces (Fig. 9G–I). The surfaces have also shown excellent stability over time. Further, these surfaces have significantly reduced microbial adhesion and biofilm formation, indicating antimicrobial properties.

Movahaghi *et al.* fabricated titania nanotube surfaces *via* electrochemical anodization and titanium nanoflowers *via* hydrothermal treatment.<sup>105</sup> These surfaces were further treated with (heptadecafluoro-1,1,2,2-tetrahydrodecyl)trichlorosilane to

make them superhemophobic (*i.e.*, surfaces that display contact angles  $>150^\circ$  with blood). These surfaces upon fluorination displayed an apparent contact angle of  $150^\circ$  and low rolloff angles for human blood plasma, indicating superhemophobicity. These surfaces displayed significant lower adhesion and activation of platelets when compared to hemophobic and hemophilic surfaces (Fig. 9J–L). Bartlet *et al.* also developed superhemophobic titania nanotube surfaces.<sup>106</sup> The titania nanotube arrays were developed by the anodizing technique and these surfaces were made superhemophobic by vapor phase silanization. These surfaces showed lower protein adsorption and lower platelet adhesion/activation, indicating a promising approach to design hemocompatible materials.

Montomerie *et al.* fabricated superhydrophobic titania nanoflowers *via* a hydrothermal process and silanization using the Ti-6Al-4V alloy.<sup>107</sup> These surfaces showed significantly reduced protein adsorption and platelet adhesion and activation. The superhydrophobic titania nanoflowers indicated improved hemocompatibility and reduced bacterial adhesion when compared to both non-textured and unmodified Ti-6Al-4V surfaces.

Moradi *et al.* investigated the effect of wettability on the blood compatibility of titanium and stainless steel substrates.<sup>108</sup> They examined different surface chemistries and micro/nanostructures to study their effect on protein adsorption and platelet adhesion. The wettability of the surfaces was modified using different chemical treatments and laser ablation methods. They concluded that a carbonized superhydrophobic cauliflower-like pattern was more resistant to protein and platelet adhesion when compared to other superhydrophobic surfaces, possibly because of the stability in the Cassie–Baxter state. In addition, the results showed that, in the hydrophilic regime, a higher roughness corresponds to increased platelet adhesion due to the larger blood–surface contact area.

**4.2.5 Bioactive surfaces.** The modification of titanium surfaces using bioactive molecules or biopolymers, such as polysaccharides, peptides, and antibodies, has received great attention to enhance their hemocompatibility properties. Biopolymers, such as heparin, chitosan, and some zwitterionic polymers, have been widely used to prevent protein and platelet attachments. Heparin is a naturally occurring polysaccharide and the most used antithrombogenic agent.<sup>57</sup> It possesses a very similar structure to heparan sulfate, a proteoglycan present on the endothelial cell surface that provides the natural anticoagulant surface properties of the endothelium.<sup>109</sup> Heparin is responsible for binding to antithrombin and inhibiting fibrin mesh formation. Because heparin is a highly negatively charged molecule, it is usually incorporated on titanium surfaces *via* electrostatic interactions with positively charged polymers to avoid the reduction of its biological activity.<sup>110</sup> Heparin has been combined with different polycations such as chitosan, tanfloc, and collagen to coat titanium using the layer-by-layer (LbL) self-assembly technique.<sup>111,112</sup>

Zhang *et al.* showed that collagen/heparin coating on titanium surfaces decreases the platelet adhesion and activation

and improves the endothelialization process of the implant.<sup>113</sup> Collagen is the major component of the extracellular matrix (ECM) and has been used to modify the surface of cardiovascular implants to enhance the biocompatibility and induce cell–biomaterial interactions.<sup>111</sup> Cherng *et al.* coated pure titanium surfaces with heparin/dopamine and heparin/collagen *via* LbL techniques.<sup>114</sup> Heparin/dopamine was a porous polymer structure and heparin/collagen was a multilayer structure constructed by electrolytes. Both these surfaces promoted the anticoagulation effect when compared to actual surfaces. However, the anticoagulation effect was better on the heparin/dopamine coated surfaces due to its long-term stability.<sup>115</sup>

Yang *et al.* loaded TiO<sub>2</sub> nanotube arrays with a 5-layer polydopamine coating and further coated the surface with the anticoagulant drug bivalirudin. The polydopamine coating controlled the release kinetics of bivalirudin and the bivalirudin activity was seen for more than 300 days compared to the 40-day activity from TiO<sub>2</sub> nanotubes loaded with the bivalirudin substrate. *In vitro* and *ex vivo* studies showed that the modified surface improved hemocompatibility by reducing adhesion and denaturation of fibrinogen and platelets and effectively reducing thrombus formation.<sup>116</sup>

Li *et al.* developed co-immobilization to form heparin and fibronectin films on aminosilanized titanium surfaces.<sup>117</sup> This technique combines electrostatic interaction and co-immobilization, and the co-immobilized films were stable after immersion in phosphate-buffered saline (PBS) for five days and enhanced the hemocompatibility of titanium surfaces. Fibronectin is an adhesive glycoprotein that promotes endothelial cell attachment and spreading.<sup>118</sup> The films reduced the hemolysis rate, prolonged the blood coagulation time, and increased the ATIII binding density. The co-immobilized surfaces also showed less platelet activation and aggregation, and less fibrinogen conformational change in comparison with the unmodified titanium surface. Similarly, Li *et al.* fabricated titanium surfaces with heparin/fibronectin complexes. The heparin and fibronectin mixture was covalently immobilized on a titanium substrate and showed improved hemocompatibility and endothelialization.<sup>119</sup> The surfaces reduced the blood hemolysis rate, prolonged the blood coagulation time, decreased platelet activation and aggregation, and induced less fibrinogen conformational change when compared with the unmodified titanium surface.

Xu and Cai prepared a bioactive coating by self-assembly of phase transited lysozyme (PTL) and heparin to improve the biocompatibility of titanium.<sup>120</sup> PTL has been shown to have excellent biocompatibility and antibacterial properties, and in this study positively charged PTL was used for strong electrostatic interactions with heparin. The PTL/heparin coated surfaces were hydrophilic in nature. The results indicated that these surfaces showed adhesion of a lower number of platelets and a delayed blood clotting time when compared to other surfaces (Fig. 10A–C). These surfaces also showed a low hemolysis ratio, indicating their better hemocompatibility compared to other surfaces.

Another biopolymer largely employed to introduce cell recognition sites to the biomaterial surface is chitosan.



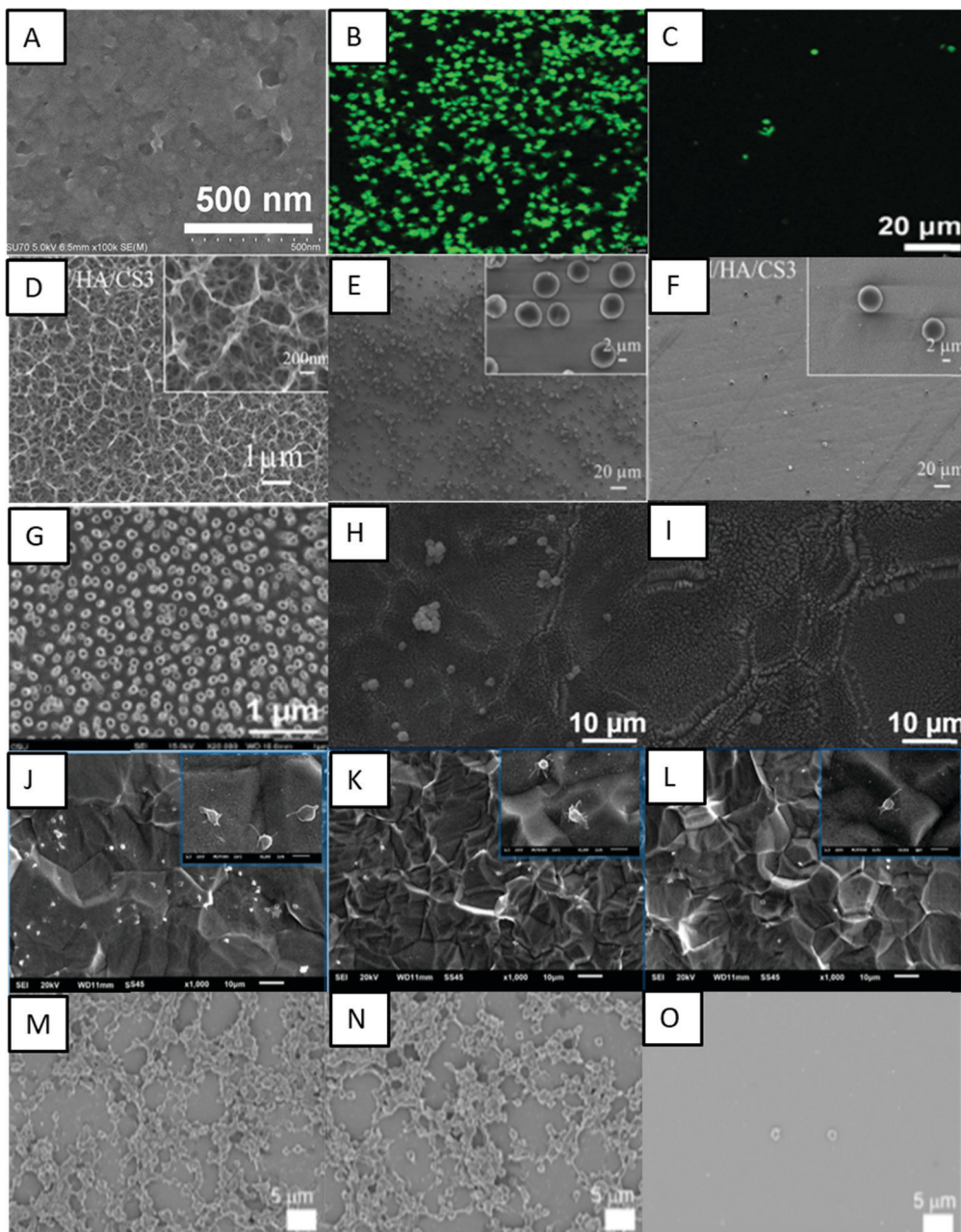


**Fig. 10** (A) SEM image showing the surface microtopography of a titanium surface modified with PTL/heparin. (B and C) Fluorescence images showing the adhesion of platelets on bare titanium and titanium modified with PTL/heparin, respectively.<sup>120</sup> Adapted with permission from ref. 120. Copyright 2019, Elsevier. (D) SEM images showing the morphology of titanium surfaces modified with heparin/chitosan. (E and F) SEM images showing platelet adhesion on titanium and titanium surfaces modified with heparin/chitosan, respectively.<sup>112</sup> Adapted with permission from ref. 112. Copyright 2018, Elsevier. (G) SEM image showing titania nanotube surfaces modified with tanfloc/heparin polyelectrolyte multilayers. (H and I) SEM images showing platelet adhesion on unmodified titania nanotube surfaces and titania nanotube surfaces modified with tanfloc/heparin, respectively.<sup>110</sup> Adapted with permission from ref. 110. Copyright 2020, Wiley-VCH. (J-L) SEM images showing platelet adhesion on pristine titanium, TA/SS 1, and TA/SS 2 coated surfaces – 1 and 2 indicating different volume ratios.<sup>126</sup> Adapted with permission from ref. 126. Copyright 2020, Elsevier. (M-O) SEM images showing platelet adhesion on non-treated, tannic acid-treated, and ulvan-coated Ti/TiO<sub>2</sub> surfaces, respectively.<sup>128</sup> Adapted with permission from ref. 128. Copyright 2020, Elsevier.

Chitosan has excellent biocompatibility properties, and its positive charge allows it to be combined with heparin *via* the LbL technique. Zhang *et al.* investigated the immobilization of heparin and chitosan on titanium to improve hemocompatibility and antibacterial activity (Fig. 10D-F).<sup>112</sup> They showed that these

surfaces were able to prevent protein absorption, platelet adhesion, and blood clot mass. Vyas *et al.* also developed biofunctionalization of titanium with chitosan/hydroxyapatite *via* silanization.<sup>121</sup> Hydroxyapatite is a bioactive ceramic largely used for biomaterial applications due to its similarity with natural bone.<sup>122</sup> These



surfaces were able to significantly decrease in hemolysis percentage in comparison with cpTi.<sup>121</sup>

Zwitterionic polymers are known to be resistant to protein adsorption due to ionic interactions that rapidly create a hydration layer on the surface.<sup>69</sup> Zwitterionic molecules have equal anion and cation groups on their chains, which make them highly hydrophilic and endow them with natural antifouling properties.<sup>123</sup> Sabino *et al.* showed that the combination of a cationic tannin derivative (tanfloc) with heparin by LbL assembly significantly decreases factor XII activation, and platelet adhesion and activation.<sup>110</sup> The zwitterionic-like properties of tanfloc are able to prevent blood protein adsorption and heparin acts to inhibit the coagulation cascade activation.<sup>124</sup> They developed tanfloc/heparin polyelectrolyte multilayers on titania nanotube array surfaces to enhance blood compatibility and antibacterial properties.<sup>110</sup> The tanfloc/heparin coated nanotube arrays were hydrophilic in nature and displayed a significant decrease in fibrinogen adsorption, factor XII activation and platelet adhesion and activation (Fig. 10G–I). These surfaces also reduced bacterial adhesion and proliferation, further indicating no biofilm formation. These surfaces thus enhanced blood compatibility and antibacterial properties on titanium surfaces.

Jia *et al.* modified TiO<sub>2</sub> nanotubes with two types of zwitterionic polymers, poly(sulfobetaine methacrylate) and poly(carboxybetaine methacrylate), using the atom transfer radical polymerization technique.<sup>125</sup> Both polymer brushes reduced adsorption of albumin and fibrinogen protein to the surface compared to TiO<sub>2</sub> nanotubes. The FTIR results showed that the adsorbed albumin on the polymer coated surface had a significantly different secondary structure, which reduced platelet adhesion and activation. In contrast, the adsorbed albumin on the TiO<sub>2</sub> nanotube surface showed no structural changes.<sup>125</sup>

Cheng *et al.* conjugated natural tannic acid (TA) and silk sericin (SS) *via* hydrogen bonding interactions and the resulting TA/SS conjugates were deposited on the titanium surfaces through surface adhesive trihydroxyphenyl groups in TA.<sup>126</sup> TA and its derivatives are widely used as primers for immobilization of other molecules due to the presence of phenolic hydroxyl groups that could act as hydrogen bond donors.<sup>127</sup> The TA/SS coated surfaces were hydrophilic in nature. These surfaces were repellent to proteins and showed lower platelet adhesion and anti-adhesive bacterial properties (Fig. 10J–L). These surfaces further showed low cytotoxicity towards fibroblast cells indicating overall biocompatibility.

Lee and Kang used a green seaweed derived polysaccharide ulvan to enhance the blood compatibility of Ti/TiO<sub>2</sub> surfaces.<sup>128</sup> Tannic acid was used for surface coating and subsequent grafting of ulvan onto the surface. Ulvan is a sulfated polysaccharide which has recently attracted attention due to its antioxidant, antiviral, and anti-adhesive properties.<sup>129</sup> The results indicated that the ulvan coated surfaces were superhydrophilic in nature and resulted in a significant reduction in fibrinogen adsorption and platelet adhesion, thus enhancing hemocompatibility (Fig. 10M–O).

Chen *et al.* prepared functional titanium surfaces with carboxylic terminated PEG<sub>600</sub>/PEG<sub>400</sub> and CD34 antibodies

and evaluated those surfaces for hemocompatibility.<sup>130</sup> The titanium surfaces were initially hydroxylated and further aminosilanized which were further used for covalent grafting of polyethylene glycol and the antibody. The CD34 antibody was immobilized on the surface to attract endothelial progenitor cells (EPCs) directly from the bloodstream.<sup>130</sup> The *in vitro* platelet adhesion tests confirmed superior hemocompatibility and enhanced endothelialization when compared to control surfaces.

Wu *et al.* fabricated quercetin-loaded chitosan nanoparticles and using the LbL self-assembly technique coated titanium substrates with five and ten bilayers of hyaluronan and quercetin-loaded chitosan nanoparticles.<sup>131</sup> Quercetin is a naturally occurring flavonoid that has been shown to exert the anticoagulant effect similar to heparin. The 10-bilayer modified surface with quercetin-loaded chitosan as the top layer reduced platelet adhesion compared to the control titanium surface and the 5-bilayer surface with hyaluronan as the top layer. This indicates that quercetin-loaded chitosan improved anticoagulation.<sup>131</sup>

Llopis-Grimalt *et al.* modified the titanium surface to improve tissue response to stents using two different approaches, the use of nanostructuration by electrochemical anodization and the addition of quercitrin to the titanium surface.<sup>132</sup> Quercitrin, a glycoside formed from the flavonoid quercetin, has shown enhanced cell differentiation and anti-inflammatory activity when immobilized on titanium surfaces.<sup>133</sup> The surfaces were investigated for cell adhesion, cytotoxicity, nitric oxide production and metabolic activity using primary human umbilical cord endothelial cells. Platelet adhesion, hemolysis rate, and bacterial adhesion were also analyzed. The results indicated that all surfaces were biocompatible, with no hemolysis, and the nanostructured surfaces displayed lower platelet adhesion. The nanostructure surfaces coated with quercitrin also showed enhanced endothelialization and lower bacterial adhesion, and also they were able to prevent thrombosis, thus being a promising approach to improve the biocompatibility of bare metal stents.

**4.2.6 Bio-inspired surfaces.** The endothelial monolayer in blood vessels provides the perfect environment of blood compatibility. Blood flows inside them without any attraction or thrombus formation. The endothelial cells that line the interior surface of healthy blood vessels prevent blood clotting *via* several mechanisms, such as nitric oxide (NO) release or recruitment of heparan sulfate.<sup>134</sup> The endothelial inner lining is composed by a layer called glycocalyx, which is rich in proteoglycans bearing glycosaminoglycan (GAG). Recent research has been focused on creating multifunctional surfaces that can mimic the endothelium environment. Simon-Walker *et al.* coated TiO<sub>2</sub> nanotubes (TiO<sub>2</sub>NT) with heparin–chitosan polyelectrolyte multilayers (PEM) to provide glycosaminoglycan functionalization.<sup>135</sup> These surfaces were then modified with NO-donor chemistry to provide an important antithrombotic signal. The combination of surface nanotopography, GAG-based surfaces, with NO-donor chemistry demonstrated a substantial reduction in platelet adhesion and activation compared to unmodified TiO<sub>2</sub> surfaces (Fig. 11A–G).

Liu *et al.* developed a multifunctional titanium surface for simultaneous enhancement of endothelial cell selectivity and



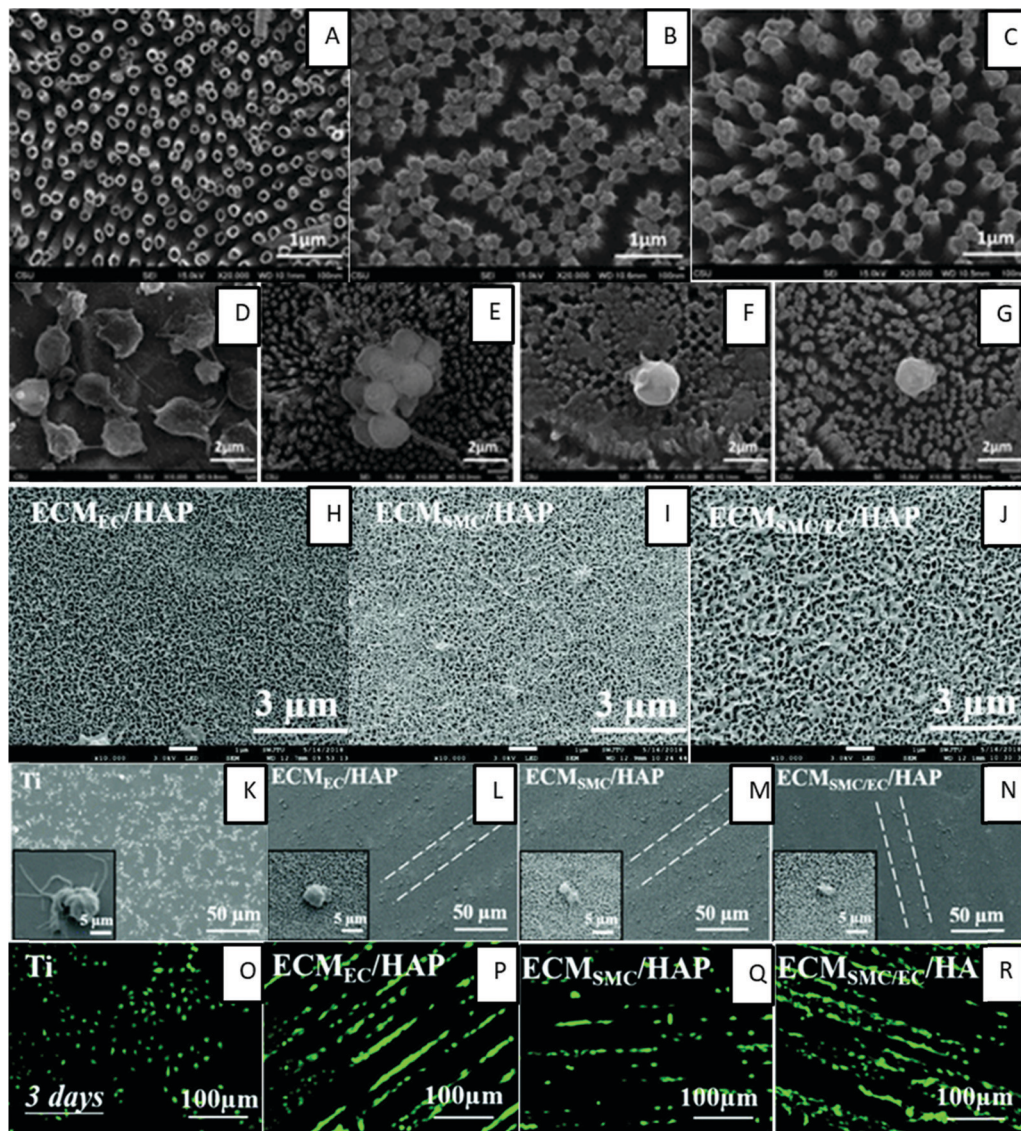


**Fig. 11** (A–C) SEM images showing  $\text{TiO}_2\text{NT}$ ,  $\text{TiO}_2\text{NT} + \text{PEM}$  and  $\text{TiO}_2\text{NT} + \text{PEM} + \text{NO}$  surfaces. (D–G) SEM images showing adhered cells on bare titanium,  $\text{TiO}_2\text{NT}$ ,  $\text{TiO}_2\text{NT} + \text{PEM}$  and  $\text{TiO}_2\text{NT} + \text{PEM} + \text{NO}$  surfaces.<sup>135</sup> Adapted with permission from ref. 135. Copyright 2017, American Chemical Society. (H–J) SEM images showing the surface morphology of HA micro-patterned titanium surfaces modified with EC-ECM ( $\text{ECM}_{\text{EC}}/\text{HAP}$ ), SMC-ECM ( $\text{ECM}_{\text{SMC}}/\text{HAP}$ ), and both SMC-ECM and EC-ECM ( $\text{ECM}_{\text{SMC/EC}}/\text{HAP}$ ), respectively.<sup>137</sup> (K–N) SEM images showing platelet adhesion on respective surfaces.<sup>137</sup> (O–R) Fluorescence images showing the growth of HUVECs after 3 days on respective surfaces.<sup>137</sup>

hemocompatibility. The surface was prepared by conjugation of the REDV peptide to a surface grafted PEGMA polymer brush *via* surface-initiated atom transfer radical polymerization on a dopamine-modified titanium surface.<sup>136</sup> This surface showed improved endothelial cell selectivity and hemocompatibility, with reduced platelet adhesion when compared to pristine titanium.

Han *et al.* prepared a nature inspired extracellular matrix (ECM) coating on a titanium surface by culturing/deculturing smooth muscle cells (SMC) and endothelial cells (EC) controlled by the hyaluronic acid (HA) micro-pattern.<sup>137</sup> This double deck ECM coating showed a higher ECM density, a different wettability and larger pore sizes which lead to better hemocompatibility, anti-inflammation, tissue compatibility and

pro-endothelialization (Fig. 11H–R). The ECM coating maximized the reproducibility of the structure and functionality of the vascular basement membrane.

Wang *et al.* also prepared an ECM inspired surface by functionalization with heparin, fibronectin, and VEGF on titanium surfaces to construct a multifunctional microenvironment to inhibit thrombus formation.<sup>138</sup> The modified surfaces significantly enhanced the ATIII binding density and prolonged the clotting time. The *in vitro* platelet study also indicated favorable anticoagulant properties, thus indicating that the heparin/fibronectin/VEGF multifunctional coating was successfully constructed with desirable anticoagulant properties. In addition, these surfaces promoted enhanced proliferation of EPCs and ECs, thus accelerating endothelialization.

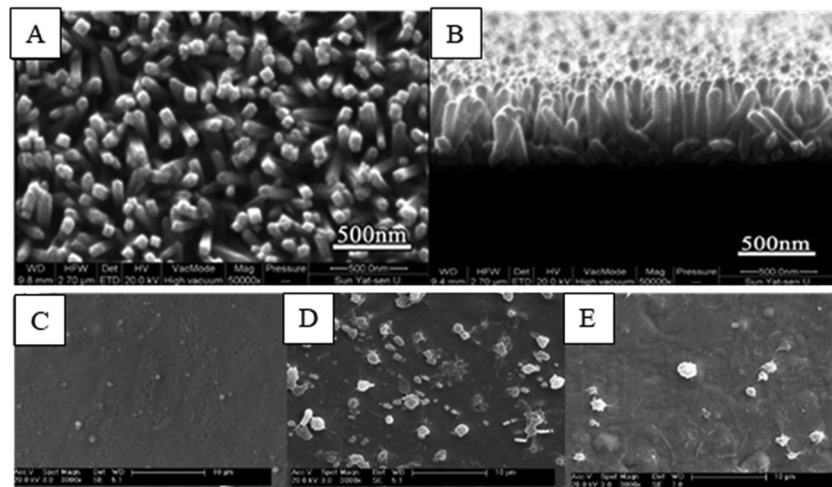


Fig. 12 (A and B) SEM images showing the surface morphology of rutile TiO<sub>2</sub> nanorod arrays (TNA).<sup>139</sup> (C) SEM images showing the surface morphology of the ZrN film. (D and E) SEM images showing platelet adhesion on nickel–titanium SMA and ZrN film surfaces, respectively.<sup>141</sup> Adapted with permission from ref. 141. Copyright 2010, Elsevier.

**4.2.7 Other surface modifications.** Several other agents have also been incorporated on the titanium surface to enhance its hemocompatibility.<sup>60</sup> Some cardiovascular implants, such as mechanical heart valves and stents, have been coated with pyrolytic carbon, which is known to decrease platelet adhesion and activation.<sup>3</sup> Chen *et al.* fabricated TiO<sub>2</sub> nanorod arrays (TNA) and used magnetic filtered cathodic vacuum arc deposition (FCVAD) to deposit carbon plasma nanocoating with sp<sup>3</sup>-C bonding on these nanorod arrays (Fig. 12A and B).<sup>139</sup> The TNA nanocomposites were investigated for hemocompatibility and cell endothelialization. The carbon nanocoatings improved cell viability and possessed higher hemocompatibility. Their previous work also indicated that these TNAs showed excellent blood compatibility, showing drastically reduced platelet adhesion and activation due to hydrophobicity and surface topography.<sup>140</sup>

Chu *et al.* deposited zirconium nitride (ZrN) films on an electro-polished nickel–titanium shape memory alloy (SMA). The ZrN film displayed a fine fibrous structure composed of a stable ZrN phase together with a small amount of a second ZrO<sub>2</sub> phase.<sup>141</sup> The results indicated that the ZrN films improved hemolysis resistance and thromboresistance, thereby making the treated surface materials more suitable for blood-contacting implants (Fig. 12C–E).

Cattaneo *et al.* investigated the *in vitro* biocompatibility of braided electropolished/blue oxide nickel–titanium samples in a blood flow loop which showed significantly lower platelet adhesion.<sup>142</sup> Further there was a significant increase in cell seeding when compared to non-electropolished surfaces with a native oxide surface. The results concluded the presence of a thin layer mainly containing titanium oxynitride as a potential cause of improved biological performance.

## 5. Conclusions and future perspectives

Blood is a complex smart liquid which can perform various necessary functions needed for our body functionality.

However, one of its main properties is to clot when exposed to a foreign environment/material and this property poses a major concern when an implant is introduced into the human body. Hence, researchers have been exploring different techniques to enhance the hemocompatibility of implant surfaces. Design of hemocompatible titanium surfaces can be achieved by understanding the blood kinetics and the series of reactions taking place due to blood proteins, cells, and platelets which lead to thrombus formation and inflammation. The influence of implant surface properties such as chemistry, morphology, crystallinity, charge, and wettability has been shown to be significant, and various studies have been carried out to develop surfaces with improved hemocompatibility.

Different techniques for surface modification reviewed in this manuscript have shown that hemocompatibility can be improved with surfaces imitating the vascular environment with surface morphology/chemistry, repelling the blood–protein interaction, anticoagulant drug loading and NO release. However, it is noticed that the combination of these properties enhances hemocompatibility significantly. The key aspects to be more focused upon are the durability and longevity of the surface modification, commercialization potential and more realistic testing methods.

Hundreds of new surface modification techniques are proposed, studied, and published annually. However, most of the studies focus on the evaluation of platelet adhesion and activation, protein adsorption, and hemolysis and coagulation tests. It is critical that researchers also investigate the contact and complement activation of the surfaces as they are important aspects of blood compatibility. In addition, most of the surfaces are evaluated in *in vitro* conditions with isolated blood components for a short duration of time. In reality, implants are present inside the human body, with blood constantly flowing over the surface for longer periods. Hence, it is important to evaluate surfaces under dynamic conditions and more *in vivo* evaluations need to be done to understand the



surface hemocompatibility. Besides that, implant surfaces are generally evaluated using human blood from healthy donors. In the current era, with advancement in biomedical sciences, implants are used by patients from different age groups, who also have other diseases or complications that can alter immune reactions to implants. Hence, it is important to perform hemocompatibility studies considering different scenarios.

Titanium will continue to play an important role in blood-contacting implants for the foreseeable future. Although titanium has proven to be an excellent material for implants, there are still significant problems such thrombosis and restenosis due to undesirable blood–surface interactions. Over the years several approaches have been proposed to enhance the surface properties of titanium-based materials to prevent thrombus formation. Some of them are based on creating micro/nano-scale topography, while others proposed surface chemistry modification. The combination of both strategies, which makes possible tailoring of the surface characteristics, such as wettability, roughness, surface charge, and crystallinity, has been shown to make the surface more compatible with blood and its components. Another promising approach is the immobilization of bioactive molecules on the titanium surface, such as polysaccharides, peptides, and antibodies, which improves the blood–biomaterial response by using agents that are similar to the ones present in the body.

Recent research has also focused on the development of multifunctional titanium surfaces with the aim to mimic the endothelial environment. By modifying these surfaces through physical, chemical, and biological processes, the biomaterial would be able to not only prevent thrombogenic and inflammatory responses, but also stimulate endothelial cell adhesion, migration, and proliferation, and eventually build an endothelial layer on the titanium surfaces. In the near future, the new generation of titanium-based biomaterials should take advantage of the current state of the art to further improve the blood–surface interaction and develop a truly hemocompatible titanium surface. We believe that this review contributed to providing guidelines for the development of new and enhanced titanium-based surfaces for blood-contacting implants.

## Conflicts of interest

There are no conflicts to declare.

## References

- 1 A. M. Khorasani, M. Goldberg, E. H. Doeven and G. Littlefair, *J. Biomater. Tissue Eng.*, 2015, **5**, 593–619.
- 2 M. T. Kalathottukaren and J. N. Kizhakkedathu, *Hemocompatibility of Biomaterials for Clinical Applications: Blood–Biomaterials Interactions*, Elsevier, 2018, pp. 29–49.
- 3 I. H. Jaffer, J. C. Fredenburgh, J. Hirsh and J. I. Weitz, *J. Thromb. Haemostasis*, 2015, **13**, S72–S81.
- 4 X. R. Xu, N. Carrim, M. A. Dias Neves, T. McKeown, T. W. Stratton, R. Matos, P. Coelho, X. Lei, P. Chen, J. Xu, X. Dai, B. X. Li and H. Ni, *Thromb. J.*, 2016, **14**, 29.
- 5 I. H. Jaffer and J. I. Weitz, *Acta Biomater.*, 2019, **94**, 2–10.
- 6 J. L. Brash, T. A. Horbett, R. A. Latour and P. Tengvall, *Acta Biomater.*, 2019, **94**, 11–24.
- 7 L. P. Dasi, H. A. Simon, P. Sucosky and A. P. Yoganathan, *Clin. Exp. Pharmacol. Physiol.*, 2009, **36**, 225–237.
- 8 V. L. Gott, D. E. Alejo and D. E. Cameron, *Annals of Thoracic Surgery*, Elsevier Inc., 2003, vol. 76, pp. S2230–S2239.
- 9 G. H. Kim, D. H. Yang, J. W. Kang, D. H. Kim, S. H. Jung and T. H. Lim, *J. Cardiovasc. Comput. Tomogr.*, 2016, **10**, 191–192.
- 10 N. Uriel, J. Han, K. A. Morrison, N. Nahumi, M. Yuzefpolkskaya, A. R. Garan, J. Duong, P. C. Colombo, H. Takayama, S. Thomas, Y. Naka and U. P. Jorde, *J. Heart Lung Transplant.*, 2014, **33**, 51–59.
- 11 M. Bakir, *J. Biomater. Appl.*, 2012, **27**, 3–15.
- 12 S. A. Smith, R. J. Travers and J. H. Morrissey, *Crit. Rev. Biochem. Mol. Biol.*, 2015, **50**, 326–336.
- 13 N. Mackman, *Nature*, 2008, **451**, 914–918.
- 14 V. K. Manivasagam and K. C. Popat, *Mater. Sci. Eng., C*, 2021, **128**, 112315.
- 15 J. Vishnu, V. K. Manivasagam, V. Gopal, C. Bartomeu Garcia, P. Hameed, G. Manivasagam and T. J. Webster, *Nanomedicine*, 2019, **20**, 102016.
- 16 H. J. Rack and J. I. Qazi, *Mater. Sci. Eng., C*, 2006, **26**, 1269–1277.
- 17 F. Zhang, Z. Zhang, X. Zhu, E. T. Kang and K. G. Neoh, *Biomaterials*, 2008, **29**, 4751–4759.
- 18 S. Lee, Y. Y. Chang, J. Lee, S. K. Madhurakkat Perikamana, E. M. Kim, Y. H. Jung, J. H. Yun and H. Shin, *Biomater. Sci.*, 2020, **8**, 3404–3417.
- 19 M. Kulkarni, A. Mazare, E. Gongadze, S. Perutkova, V. Kralj-Iglc, I. Milošev, P. Schmuki, A. Iglić and M. Mozetić, *Nanotechnology*, 2015, **26**, 062002.
- 20 M. Kaur and K. Singh, *Mater. Sci. Eng., C*, 2019, **102**, 844–862.
- 21 A. Dehghanianhadikolaei, H. Ibrahim, A. Amerinatanzi, M. Hashemi, N. S. Moghaddam and M. Elahinia, *J. Mater. Sci.*, 2019, **54**, 7333–7355.
- 22 A. T. Sidambe, *Materials*, 2014, **7**, 8168–8188.
- 23 N. Eliaz, *Materials*, 2019, **12**, 407.
- 24 R. Zhang, X. Ai, Y. Wan, Z. Liu, D. Zhang and S. Feng, *Int. J. Corros.*, 2015, **2015**, 1–8.
- 25 J. C. M. Souza, M. B. Sordi, M. Kanazawa, S. Ravindran, B. Henriques, F. S. Silva, C. Aparicio and L. F. Cooper, *Acta Biomater.*, 2019, **94**, 112–131.
- 26 G. Wang, J. Li, K. Lv, W. Zhang, X. Ding, G. Yang, X. Liu and X. Jiang, *Sci. Rep.*, 2016, **6**, 1–13.
- 27 M. L. Teffo, N. E. Nyakane, M. Seerane, M. B. Shongwe and R. Machaka, *Materials Today: Proceedings*, Elsevier, 2021, vol. 38, pp. 1203–1208.
- 28 D. Banerjee and J. C. Williams, *Acta Mater.*, 2013, **61**, 844–879.
- 29 E. Alabot, D. Barba, M. R. Shagiev, M. A. Murzinova, R. M. Galeyev, O. R. Valiakhmetov, A. F. Aletdinov and R. C. Reed, *Acta Mater.*, 2019, **178**, 275–287.



30 Y. Oshida, *Bioscience and Bioengineering of Titanium Materials*, Elsevier, 2013, pp. 9–34.

31 Y. Li, C. Yang, H. Zhao, S. Qu, X. Li and Y. Li, *Materials*, 2014, **7**, 1709–1800.

32 M. Özcan and C. Hämmерle, *Materials*, 2012, **5**, 1528–1545.

33 B. S. Smith, S. Yoriya, L. Grissom, C. A. Grimes and K. C. Popat, *J. Biomed. Mater. Res., Part A*, 2010, **95**, 350–360.

34 V. B. Damodaran, D. Bhatnagar, V. Leszczak and K. C. Popat, *RSC Adv.*, 2015, **5**, 37149–37171.

35 Y. Cheng, H. Yang, Y. Yang, J. Huang, K. Wu, Z. Chen, X. Wang, C. Lin and Y. Lai, *J. Mater. Chem. B*, 2018, **6**, 1862–1886.

36 V. Balan and L. Verestiuc, *Eur. Polym. J.*, 2014, **53**, 171–188.

37 M. B. Gorbet and M. V. Sefton, *Biomater. Silver Jubil. Compend.*, 2004, **25**, 219–241.

38 L. Chen, D. Han and L. Jiang, *Colloids Surf., B*, 2011, **85**, 2–7.

39 H. S. Lee, N. Tomczyk, J. Kandel, R. J. Composto and D. M. Eckmann, *J. Mater. Chem. B*, 2013, **1**, 6382–6391.

40 L. C. Xu, J. W. Bauer and C. A. Siedlecki, *Colloids Surf., B*, 2014, **124**, 49–68.

41 C. J. Wilson, R. E. Clegg, D. I. Leavesley and M. J. Pearcy, *Tissue Eng.*, 2005, **11**, 1–18.

42 P. Roach, D. Farrar and C. C. Perry, *J. Am. Chem. Soc.*, 2005, **127**, 8168–8173.

43 S. Y. Jung, S. M. Lim, F. Albertorio, G. Kim, M. C. Gurau, R. D. Yang, M. A. Holden and P. S. Cremer, *J. Am. Chem. Soc.*, 2003, **125**, 12782–12786.

44 X. Liu, L. Yuan, D. Li, Z. Tang, Y. Wang, G. Chen, H. Chen and J. L. Brash, *J. Mater. Chem. B*, 2014, **2**, 5709–5926.

45 L. C. Xu, J. W. Bauer and C. A. Siedlecki, *Colloids Surf., B*, 2014, **124**, 49–68.

46 C. Sperling, M. Fischer, M. F. Maitz and C. Werner, *Biomaterials*, 2009, **30**, 4447–4456.

47 Z. Guo, K. M. Bussard, K. Chatterjee, R. Miller, E. A. Vogler and C. A. Siedlecki, *Biomaterials*, 2006, **27**, 796–806.

48 R. M. Sabino, K. Kauk, S. Movafaghi, A. Kota and K. C. Popat, *Nanomedicine: NBM*, 2019, **21**, 102046.

49 A. De Mel, B. G. Cousins and A. M. Seifalian, *Int. J. Biomater.*, 2012, 1–8.

50 K. Chatterjee, Z. Guo, E. A. Vogler and C. A. Siedlecki, *J. Biomed. Mater. Res., Part A*, 2009, **90**, 27–34.

51 J. L. Brash, T. A. Horbett, R. A. Latour and P. Tengvall, *Acta Biomater.*, 2019, **94**, 11–24.

52 M. Gorbet, C. Sperling, M. F. Maitz, C. A. Siedlecki, C. Werner and M. V. Sefton, *Acta Biomater.*, 2019, **94**, 25–32.

53 F. Poppelaars, B. Faria, M. G. da Costa, C. F. M. Franssen, W. J. van Son, S. P. Berger, M. R. Daha and M. A. Seelen, *Front. Immunol.*, 2018, **9**, 71.

54 Y. Yan, L. C. Xu, E. A. Vogler and C. A. Siedlecki, *Hemocompatibility of Biomaterials for Clinical Applications: Blood–Biomaterials Interactions*, Elsevier, 2018, pp. 3–28.

55 A. Thor, L. Rasmusson, A. Wennerberg, P. Thomsen, J.-M. Hirsch, B. Nilsson and J. Hong, *Biomaterials*, 2007, **28**, 966–974.

56 X. R. Xu, N. Carrim, M. A. D. Neves, T. McKeown, T. W. Stratton, R. M. P. Coelho, X. Lei, P. Chen, J. Xu, X. Dai, B. X. Li and H. Ni, *Thromb. J.*, 2016, **14**, 29.

57 R. Biran and D. Pond, *Adv. Drug Delivery Rev.*, 2017, **112**, 12–23.

58 M. Gorbet, C. Sperling, M. F. Maitz, C. A. Siedlecki, C. Werner and M. V. Sefton, *Acta Biomater.*, 2019, **94**, 25–32.

59 Y. K. Kim, E. Y. Chen and W. F. Liu, *J. Mater. Chem. B*, 2016, **4**, 1600–1609.

60 V. Balan and L. Verestiuc, *Eur. Polym. J.*, 2014, **53**, 171–188.

61 U. T. Seyfert, V. Biehl and J. Schenk, *Biomolecular Engineering*, Elsevier, 2002, vol. 19, pp. 91–96.

62 L. Y. C. Madruga, R. M. Sabino, E. C. G. Santos, K. C. Popat, R. de, C. Balaban and M. J. Kipper, *Int. J. Biol. Macromol.*, 2020, **152**, 483–491.

63 R. Sabino and K. Popat, *Bio-Protoc.*, 2020, **10**, e3505.

64 P. Gill, V. Musaramthota, N. Munroe, A. Datye, R. Dua, W. Haider, A. McGoron and R. Rokicki, *Mater. Sci. Eng., C*, 2015, **50**, 37–44.

65 B. S. Smith and K. C. Popat, *J. Biomed. Nanotechnol.*, 2012, **8**(4), 642–658.

66 J. L. Chen, Q. L. Li, J. Y. Chen, C. Chen and N. Huang, *Appl. Surf. Sci.*, 2009, **255**, 6894–6900.

67 S. Nie, H. Qin, C. Cheng, W. Zhao, S. Sun, B. Su, C. Zhao and Z. Gu, *J. Mater. Chem. B*, 2014, **2**, 4911–4921.

68 S. Kumar, *Comprehensive Materials Processing*, Elsevier Ltd, 2014, vol. 10, pp. 93–134.

69 X. Liu, L. Yuan, D. Li, Z. Tang, Y. Wang, G. Chen, H. Chen and J. L. Brash, *J. Mater. Chem. B*, 2014, **2**, 5709–5926.

70 A. K. Kota, G. Kwon and A. Tuteja, *NPG Asia Mater.*, 2014, **6**, 109.

71 K. Y. Yeh, L. J. Chen and J. Y. Chang, *Langmuir*, 2008, **24**, 245–251.

72 B. M. L. Koch, A. Amirfazli and J. A. W. Elliott, *J. Phys. Chem. C*, 2014, **118**, 18554–18563.

73 S. Movafaghi, W. Wang, D. L. Bark, L. P. Dasi, K. C. Popat and A. K. Kota, *Mater. Horiz.*, 2019, **6**, 1596–1610.

74 D. L. Bark, H. Vahabi, H. Bui, S. Movafaghi, B. Moore, A. K. Kota, K. Popat and L. P. Dasi, *Ann. Biomed. Eng.*, 2017, **45**, 452–463.

75 K. M. Hansson, S. Tosatti, J. Isaksson, J. Wetterö, M. Textor, T. L. Lindahl and P. Tengvall, *Biomaterials*, 2005, **26**, 861–872.

76 C. J. Pan, Y. H. Hou, B. Bin Zhang, Y. X. Dong and H. Y. Ding, *J. Mater. Chem. B*, 2014, **2**, 892–902.

77 J. Herzberger, K. Niederer, H. Pohlitz, J. Seiwert, M. Worm, F. R. Wurm and H. Frey, *Chem. Rev.*, 2016, **116**, 2170–2243.

78 A. Rosengren and S. Oscarsson, *Cellular Response to Biomaterials*, Elsevier Ltd, 2008, pp. 538–559.

79 D. A. H. Hanaor and C. C. Sorrell, *J. Mater. Sci.*, 2011, **46**, 855–874.

80 F. Parrino, F. R. Pomilla, G. Camera-Roda, V. Loddo and L. Palmisano, *Titanium Dioxide ( $TiO_2$ ) and Its Applications*, Elsevier, 2021, pp. 13–66.

81 H. N. Pantaroto, J. M. Cordeiro, L. T. Pereira, A. B. de Almeida, F. H. Nociti Junior, E. C. Rangel, N. F. Azevedo



Neto, J. H. D. da Silva and V. A. R. Barão, *Mater. Sci. Eng. C*, 2021, **119**, 111638.

82 H.-J. Chiang, H.-H. Chou, K.-L. Ou, E. Sugiatno, M. Ruslin, R. A. Waris, C.-F. Huang, C.-M. Liu and P.-W. Peng, *Metals*, 2018, **8**, 513.

83 M. Erofeev, V. Ripenko, M. Shulepov and V. Tarasenko, *Eur. Phys. J. D*, 2017, **71**, 1–5.

84 M. Göttlicher, M. Rohnke, A. Kunz, J. Thomas, R. A. Henning, T. Leichtweiß, T. Gemming and J. Janek, *Solid State Ionics*, 2016, **290**, 130–139.

85 D. Xie, G. Wan, M. F. Maitz, Y. Lei, N. Huang and H. Sun, *Nucl. Instrum. Methods Phys. Res., Sect. B*, 2012, **289**, 91–96.

86 W. C. Hung, F. M. Chang, T. Sen Yang, K. L. Ou, C. T. Lin and P. W. Peng, *Mater. Sci. Eng., C*, 2016, **68**, 523–529.

87 M. Klein, Y. Kuhn, E. Woelke, T. Linde, C. Ptock, A. Kopp, T. Bletek, T. Schmitz-Rode, U. Steinseifer, J. Arens and J. C. Clauser, *Artif. Organs*, 2020, **44**, 419–427.

88 P. Hameed, V. K. Manivasagam, M. Sankar, K. C. Popat and G. Manivasagam, *Nanofibers and nanosurfaces*, Springer, Singapore, 2021, pp. 107–130.

89 C. L. Wong, Y. N. Tan and A. R. Mohamed, *J. Environ. Manage.*, 2011, **92**, 1669–1680.

90 J. Vishnu, M. Calin, S. Pilz, A. Gebert, B. Kaczmarek, M. Michalska-Sionkowska, V. Hoffmann and G. Manivasagam, *Surf. Coat. Technol.*, 2020, **396**, 125965.

91 V. K. Manivasagam and K. C. Popat, *ACS Omega*, 2020, **5**, 8108–8120.

92 Y. Cheng, H. Yang, Y. Yang, J. Huang, K. Wu, Z. Chen, X. Wang, C. Lin and Y. Lai, *J. Mater. Chem. B*, 2018, **6**, 1862–1886.

93 K. M. Kummer, E. Taylor and T. J. Webster, *Nanosci. Nanotechnol. Lett.*, 2012, **4**, 483–493.

94 I. Junkar, M. Kulkarni, M. Benčina, J. Kovač, K. Mrak-Poljšak, K. Lakota, S. Sodin-Šemrl, M. Mozetič and A. Iglič, *ACS Omega*, 2020, **5**, 7280–7289.

95 C. Pan, Y. Hu, Z. Gong, Y. Yang, S. Liu, L. Quan, Z. Yang, Y. Wei and W. Ye, *ACS Biomater. Sci. Eng.*, 2020, **6**, 2072–2083.

96 Z. Gong, Y. Hu, F. Gao, L. Quan, T. Liu, T. Gong and C. Pan, *Colloids Surf., B*, 2019, **184**, 110521.

97 S. Movafaghi, W. Wang, D. L. Bark, L. P. Dasi, K. C. Popat and A. K. Kota, *Mater. Horiz.*, 2019, **6**, 1596–1610.

98 V. Jokinen, E. Kankuri, S. Hoshian, S. Franssila and R. H. A. Ras, *Adv. Mater.*, 2018, **30**, 1705104.

99 W. Wang, K. Lockwood, L. M. Boyd, M. D. Davidson, S. Movafaghi, H. Vahabi, S. R. Khetani and A. K. Kota, *ACS Appl. Mater. Interfaces*, 2016, **8**, 18664–18668.

100 X. Gu, Y. Zheng, Y. Cheng, S. Zhong and T. Xi, *Biomaterials*, 2009, **30**, 484–498.

101 J. Y. Jiang, J. L. Xu, Z. H. Liu, L. Deng, B. Sun, S. D. Liu, L. Wang and H. Y. Liu, *Appl. Surf. Sci.*, 2015, **347**, 591–595.

102 J. Chen, J. L. Xu, J. Huang, P. Zhang, J. M. Luo and L. Lian, *J. Mater. Sci.*, 2021, **56**, 7698–7709.

103 Y. Yang, Y. Lai, Q. Zhang, K. Wu, L. Zhang, C. Lin and P. Tang, *Colloids Surf., B*, 2010, **79**, 309–313.

104 Y. Ma, L. Jiang, J. Hu, H. Liu, S. Wang, P. Zuo, P. Ji, L. Qu and T. Cui, *ACS Appl. Mater. Interfaces*, 2020, **12**, 17155–17166.

105 S. Movafaghi, V. Leszczak, W. Wang, J. A. Sorkin, L. P. Dasi, K. C. Popat and A. K. Kota, *Adv. Healthcare Mater.*, 2017, **6**, 1600717.

106 K. Bartlet, S. Movafaghi, A. Kota and K. C. Popat, *RSC Adv.*, 2017, **7**, 35466–35476.

107 Z. Montgomerie and K. C. Popat, *Mater. Sci. Eng., C*, 2021, **119**, 111503.

108 S. Moradi, N. Hadjesfandiari, S. F. Toosi, J. N. Kizhakkedathu and S. G. Hatzikiriakos, *ACS Appl. Mater. Interfaces*, 2016, **8**, 17631–17641.

109 H. D. M. Follmann, A. F. Naves, A. F. Martins, O. Félix, G. Decher, E. C. Muniz and R. Silva, *J. Colloid Interface Sci.*, 2016, **474**, 9–17.

110 R. M. Sabino, K. Kauk, L. Y. C. Madruga, M. J. Kipper, A. F. Martins and K. C. Popat, *J. Biomed. Mater. Res., Part A*, 2020, **108**, 992–1005.

111 J. Chen, C. Chen, Z. Chen, J. Chen, Q. Li and N. Huang, *J. Biomed. Mater. Res., Part A*, 2010, **95**, 341–349.

112 X. Zhang, G. Zhang, H. Zhang, J. Li, X. Yao and B. Tang, *Colloids Surf., B*, 2018, **172**, 338–345.

113 K. Zhang, J. Y. Chen, W. Qin, J. A. Li, F. X. Guan and N. Huang, *J. Mater. Sci.: Mater. Med.*, 2016, **27**, 81.

114 W. J. Cherng, Y. H. Pan, T. C. Wu, C. C. Chou, C. H. Yeh and J. J. Ho, *Appl. Surf. Sci.*, 2019, **463**, 732–740.

115 Y. Liu, K. Ai and L. Lu, *Chem. Rev.*, 2014, **114**, 5057–5115.

116 Y. Yang, X. Li, H. Qiu, P. Li, P. Qi, M. F. Maitz, T. You, R. Shen, Z. Yang, W. Tian and N. Huang, *ACS Appl. Mater. Interfaces*, 2017, **10**, 7649–7660.

117 G. Li, P. Yang, W. Qin, M. F. Maitz, S. Zhou and N. Huang, *Biomaterials*, 2011, **32**, 4691–4703.

118 R. Daum, D. Visser, C. Wild, L. Kutuzova, M. Schneider, G. Lorenz, M. Weiss, S. Hinderer, U. A. Stock, M. Seifert and K. Schenke-Layland, *Cells*, 2020, **9**, 778.

119 G. Li, P. Yang, Y. Liao and N. Huang, *Biomacromolecules*, 2011, **12**, 1155–1168.

120 K. Xu and K. Cai, *Mater. Lett.*, 2019, **247**, 95–98.

121 V. Vyas, T. Kaur, S. Kar and A. Thirugnanam, *J. Adhes. Sci. Technol.*, 2017, **31**, 1768–1781.

122 R. M. Sabino, G. Mondini, M. J. Kipper, A. F. Martins and K. C. Popat, *Carbohydr. Polym.*, 2021, **251**, 117079.

123 W. Lin, J. Zhang, Z. Wang and S. Chen, *Acta Biomater.*, 2011, **7**, 2053–2059.

124 P. C. F. da Câmara, L. Y. C. Madruga, R. M. Sabino, J. Vlcek, R. C. Balaban, K. C. Popat, A. F. Martins and M. J. Kipper, *Mater. Sci. Eng., C*, 2020, **112**, 110919.

125 E. Jia, B. Liang, Y. Lin and Z. Su, *Nanotechnology*, 2021, **32**, 305704.

126 Y. F. Cheng, Y. H. Mei, G. Sathishkumar, Z. S. Lu, C. M. Li, F. Wang, Q. Y. Xia and L. Q. Xu, *Colloids Interface Sci. Commun.*, 2020, **35**, 100241.

127 L. Meng, K. Pan, Y. Zhu, W. Wei, X. Li and X. Liu, *ACS Biomater. Sci. Eng.*, 2018, **4**, 4122–4131.

128 A. Lee and S. M. Kang, *J. Ind. Eng. Chem.*, 2020, **82**, 228–233.

129 M. J. Stadnik and M. B. de Freitas, *Trop. Plant Pathol.*, 2014, **39**, 111–118.



130 J. Chen, J. Cao, J. Wang, M. F. Maitz, L. Guo, Y. Zhao, Q. Li, K. Xiong and N. Huang, *J. Colloid Interface Sci.*, 2012, **368**, 636–647.

131 X. Wu, C. Liu, H. Chen, Y. Zhang, L. Li and N. Tang, *Coatings*, 2020, **10**, 256.

132 M. A. Llopis-Grimalt, M. A. Forteza-Genestra, V. Alcolea-Rodríguez, J. M. Ramis and M. Monjo, *Coatings*, 2020, **10**, 907.

133 A. Córdoba, M. Satué, M. Gómez-Florit, M. Hierro-Oliva, C. Petzold, S. P. Lyngstadaas, M. L. González-Martín, M. Monjo and J. M. Ramis, *Adv. Healthcare Mater.*, 2015, **4**, 540–549.

134 R. Luo, J. Zhang, W. Zhuang, L. Deng, L. Li, H. Yu, J. Wang, N. Huang and Y. Wang, *J. Mater. Chem. B*, 2018, **6**, 5582–5595.

135 R. Simon-Walker, R. Romero, J. M. Staver, Y. Zang, M. M. Reynolds, K. C. Popat and M. J. Kipper, *ACS Biomater. Sci. Eng.*, 2017, **3**, 68–77.

136 Y. Liu, T. T. Yang Tan, S. Yuan and C. Choong, *J. Mater. Chem. B*, 2013, **1**, 157–167.

137 C. Han, X. Luo, D. Zou, J. Li, K. Zhang, P. Yang and N. Huang, *Biomater. Sci.*, 2019, **7**, 2686–2701.

138 X. Wang, T. Liu, Y. Chen, K. Zhang, M. F. Maitz, C. Pan, J. Chen and N. Huang, *Appl. Surf. Sci.*, 2014, **320**, 871–882.

139 H. Chen, N. Tang, M. Chen and D. Chen, *Nanoscale Res. Lett.*, 2016, **11**, 1–9.

140 P. Luo, Z. Huang and D. Chen, *Advanced Materials Research*, Trans Tech Publications Ltd, 2011, vol. 306–307, pp. 25–30.

141 C. L. Chu, H. L. Ji, L. H. Yin, Y. P. Pu, P. H. Lin and P. K. Chu, *Surf. Coat. Technol.*, 2010, **204**, 2841–2845.

142 G. Cattaneo, C. Bräuner, G. Siekmeyer, A. Ding, S. Bauer, M. Wohlschlögel, L. Lang, T. Hierlemann, M. Akimov, C. Schlensak, A. Schüßler, H. P. Wendel and S. Krajewski, *J. Mater. Sci.: Mater. Med.*, 2019, **30**, 1–12.

